免疫学的な恒常性の維持に寄与する材料設計

杠, 和樹

Material designs for maintenance of immunological homeostasis

Kazuki Yuzuriha

Doctor of Philosophy

Graduate School of Systems Life Sciences

Kyushu University

2020

Abstract

Material designs for maintenance of immunological homeostasis

Kazuki Yuzuriha

Doctor of Philosophy
Graduate School of Systems Life Sciences
Kyushu University
2020

Increase in the patient of diseases related to the disruption of immunological homeostasis is threatening issue worldwide. Many reasons have been proposed for the increment of the disruption of immunological homeostasis. One of the reasons is the dysbiosis of the intestinal microbiome which is caused by administration of antibiotics. To restore the disrupted immunological homeostasis, immunotherapy using an antigen is fundamental solution. However, usually this kind of therapy (desensitization) takes time for completion. In this paper, I approached the goal in two ways to maintain or restore the immunological homeostasis.

In Chapter 2, I developed vitamin-peptide conjugates as effective inducer of immunotolerance toward the antigen peptides. Here I selected ATRA and vD3 as inducer of tolerogenic dendritic cells. Selective modification of these vitamins on the N-terminus of the peptide was achieved by the scheme I developed here. The obtained conjugates

showed the functions of both vitamins and antigen peptides, i.e., anti-inflammatory effects resulting from ATRA and activation of antigen-specific T cells. The conjugates reported here can be expected to promote the induction of antigen-specific Tregs, which is essential to restore the disruption of immunological homeostasis.

In Chapter 3, I proposed an antibiotic-specific adsorbent to prevent dysbiosis caused by antibiotic treatment. Hydrophilic polyethyleneglycol-based microparticles were modified with peptide ligands in a high density which is a vancomycin-specific ligand. The microparticles showed high capacity and specificity to vancomycin and successfully captured vancomycin in vivo. The microparticles protected from the C. difficile infection induced by vancomycin-induced dysbiosis.

Table of contents

CHAPTER 1

General Introduction

1.1. Immunological homeostasis

Immunological homeostasis is the state at which immune system maintains a strong defense against pathogens, while avoiding the pathogenic consequences of inappropriate responses to non-pathogenic antigens including auto-antigens [1]. Breakdown of immunological homeostasis, in association with defects in immunoregulatory mechanisms, lead to the development of an autoimmune disease and allergy. The appearance of breakdown of immunological homeostasis is caused by dietary factor, exposure to medications, and infections. Genes of antigen presenting molecules (HLA-DR, DQ) are known to determine the susceptibility to these diseases [2–5]. Antibody dugs and antigen specific immunotherapy have been developed to restore immunological homeostasis [6,7]. These therapies work for immune cells such as antigen presenting cells (APCs), B cells and T cells to achieve immunotolerance toward non-pathogenic antigens.

1.1.1. Functions of dendritic cells in immunological homeostasis

Dendritic cells (DCs) are representative APCs of the mammalian immune system. Their function is to present treated antigens on their cell surface, which are recognized by T cells. They act as messengers between the innate and the adaptive immune systems (Fig.1.3). Immature DCs are stimulated by ligands of toll-like receptors (TLRs) such as pathogen-associated molecular patterns (PAMPs) and inflammatory cytokine, tumor necrosis factor-α (TNF-α), thereby differentiated into mature DC [8–10]. Then the maturated DCs increase the expression of MHC II and costimulatory molecules, and secrete a wide variety of pro-inflammatory cytokine such as TNF-α , IL-1 β and IL-6. Helper T cells which recognize MHC-antigens complexes presented on DCs and become activated. In contact, immature DCs compete with the above-mentioned activation of helper T cells. DCs are maintained in immature state by anti-inflammatory cytokines such as IL-10 and transforming growth factor-β (TGF-β) and immunomodulatory small molecules such as calcitriol (active form of vitamin D3) and retinoic acids [11]. The immature DCs avoid the activation of helper T cells by inducing anergic response or activating Treg [12]. Induction of Tregs via DCs is important for maitaining the immunological homeostasis.

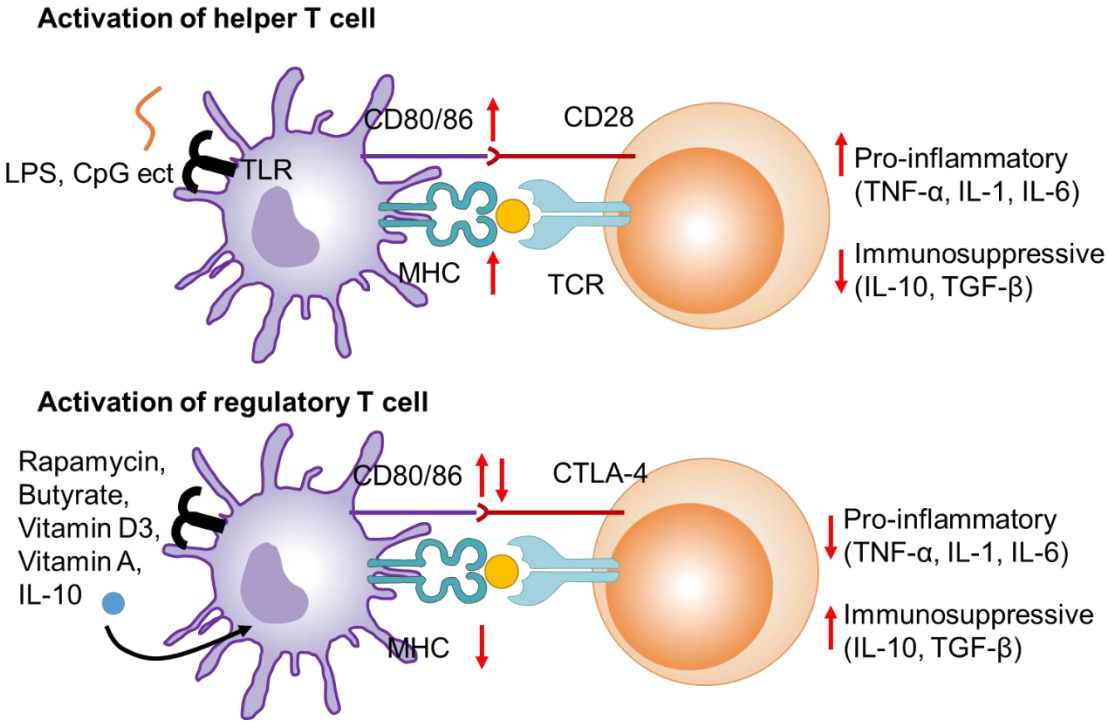

Fig. 1.1. Antigen presentation by mature and immature dendritic cell.

1.1.2. Approaches to induce immune tolerance for allergic and autoimmune diseases

Patients of allergic and autoimmune diseases are increasing worldwide [13,14]. In Japan, the number of patients with autoimmune diseases is increasing year by year, and ulcerative colitis and Parkinson's disease are the most notably increasing (Fig.1.2). And it is known that 50% of Japanese suffer from some allergy (Fig.1.3). Immunological homeostasis is disrupted in the patients; causing an excessive immune response to harmless allergens and self-tissues. Induction of antigen-specific immunotolerance is a way to recover the immunological homeostasis to treat allergies and autoimmune diseases. In the treatment of allergic diseases toward house mites and pollens, small amount allergens are administered continuously to induce allergen-specific Tregs or anergic response to allergen-specific helper T cells. However, this therapy takes long time, have risk of anaphylaxis .

To overcome the issues of conventional therapy, Kishimoto et al. reported that co-delivery of an immunomodulator and an allergen by encapsulating into nanoparticles (tNPs) improved the therapeutic effect (Fig.1.4) [17]. The nanoparticles engulfed by DCs maintain phenotype of DCs in immature state by the function of immunomodulators and promote differentiation of antigen-specific Tregs by antigen presented on DCs (Fig.1.5). They succeeded in induce immunotolerance for allergy model mice [18]. Thus, material that achieving co-delivery of immunomodulators and antigens to DCs has high potential to treat diseases in which the balance of immunological homeostasis is disrupted.

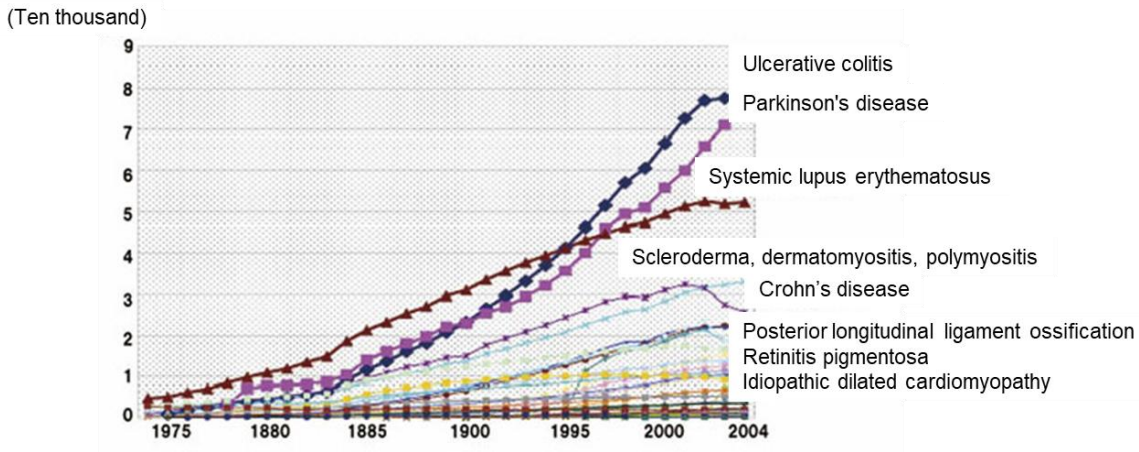

Figure. 1.2. Prevalence of autoimmune disease [15]

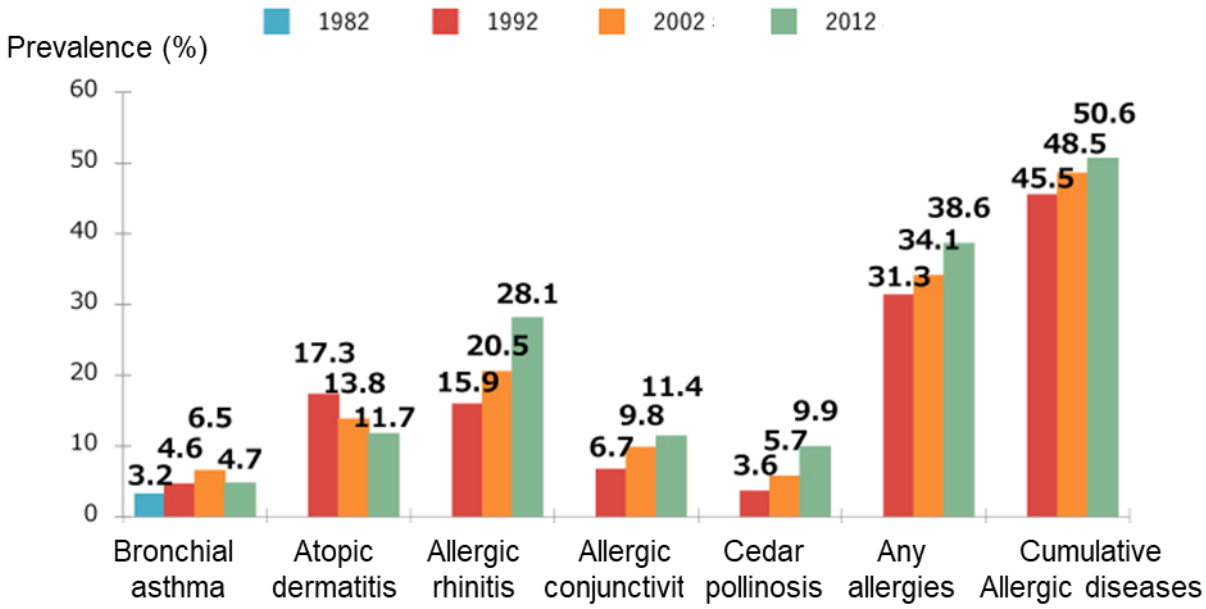

Figure. 1.3. Prevalence of allergic disease [16]

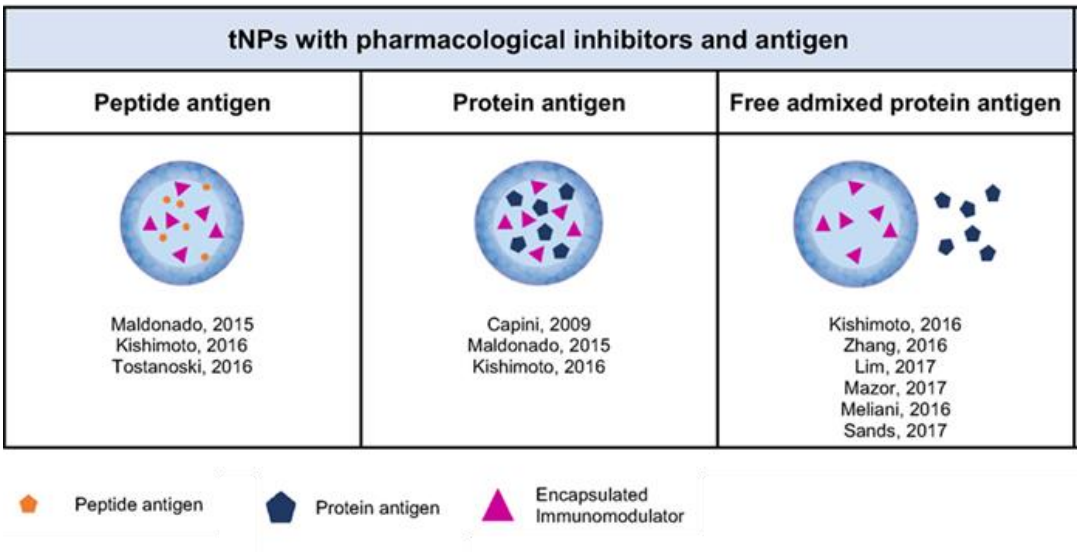

Fig. 1.4. Different types of tolerogenic nanoparticles

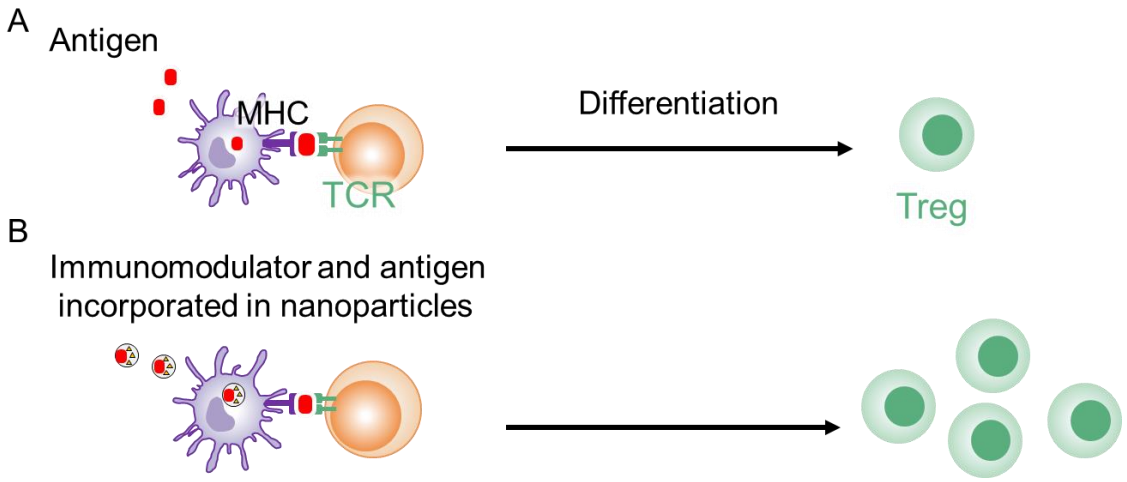

Fig. 1.5. Comparison of A) whole-allergen immunotherapy and B) tNP immunotherapy.

1.2 Contribution of microbiome to host homeostasis

Living organisms coexist with many microorganisms. In humans, there are 10 to 100 trillion microorganisms for every 10 trillion human cells [19,20]. Most of these microorganisms live in the gut. Microbiomes effectively add vast amounts of genes to the human genome, potentially increasing up to 200-fold [21]. As a result, the composition of human microbiomes can be important in health and disease situations. Commensal bacteria interact with the immune system directly or through metabolites and suppresses activities that contribute to homeostatic mechanisms (Fig.1.6). However, the pathogenic bacteria interact specifically with the immune system, disrupt homeostasis, and promote a non-immunogenic hyper-inflammatory response that promotes various gastric diseases [22]. Intestinal lymph nodes contain about 60% of systemic immune cells, and intestinal immunity is also involved in neuron and brain immune function [23,24]. Like the spleen, intestinal lymph nodes function like an organ where immunity is educated [25]. Intestinal

bacteria induce immune tolerance by metabolites produced by metabolism or by direct stimulation. For example, *Clostridium*, *Lactobacillus*, *Bifidobacterium and Bacteroides* protect mice from experimental allergies and colitis by accumulating Tregs [26–28].

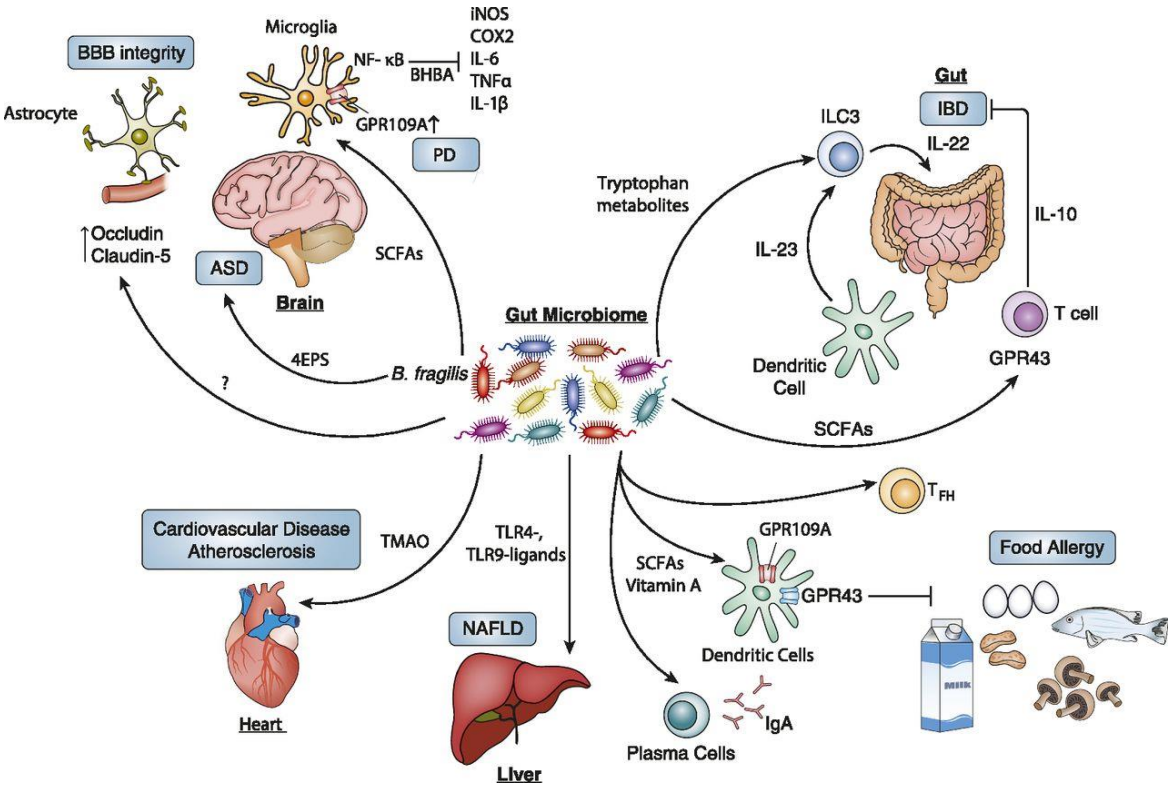

Fig. 1.6. Effect of microbiome-modulated metabolites on human health. Altered levels of microbiome-modulated metabolites have been associated with immune-mediated and immune-associated disease risk [29].

1.2.1. Dysbiosis caused by antibiotics

It is known that the intestinal flora are altered by various factors such as diet, exercise, and medication. Among them, administration of antibiotics significantly changes the composition of the intestinal flora and causes destruction (dysbiosis) of the

intestinal flora (Fig1.7) [30].

Dysbiosis caused by antibiotics reduces the number of commensal bacteria which is responsible for immune homeostasis, and increases the number of pathogenic bacteria [31]. As a result, the number of microorganisms that induce the differentiation of Tregs is reduced, so that immuological homeostasis is disrupted to cause allergies and autoimmune diseases. For example, continuous administration of vancomycin to pregnant mice resulted in excessive eosinophilia, elevated allergen-specific IgE levels, and increased airway hyper-reactivity [32]. Antibiotic treated patients also showed increased expression of IgE on basophils and IgE in serum and decreased numbers of Tregs [33]. The balance of the microbiome is one of the important factors for maintaining immunological homeostasis.

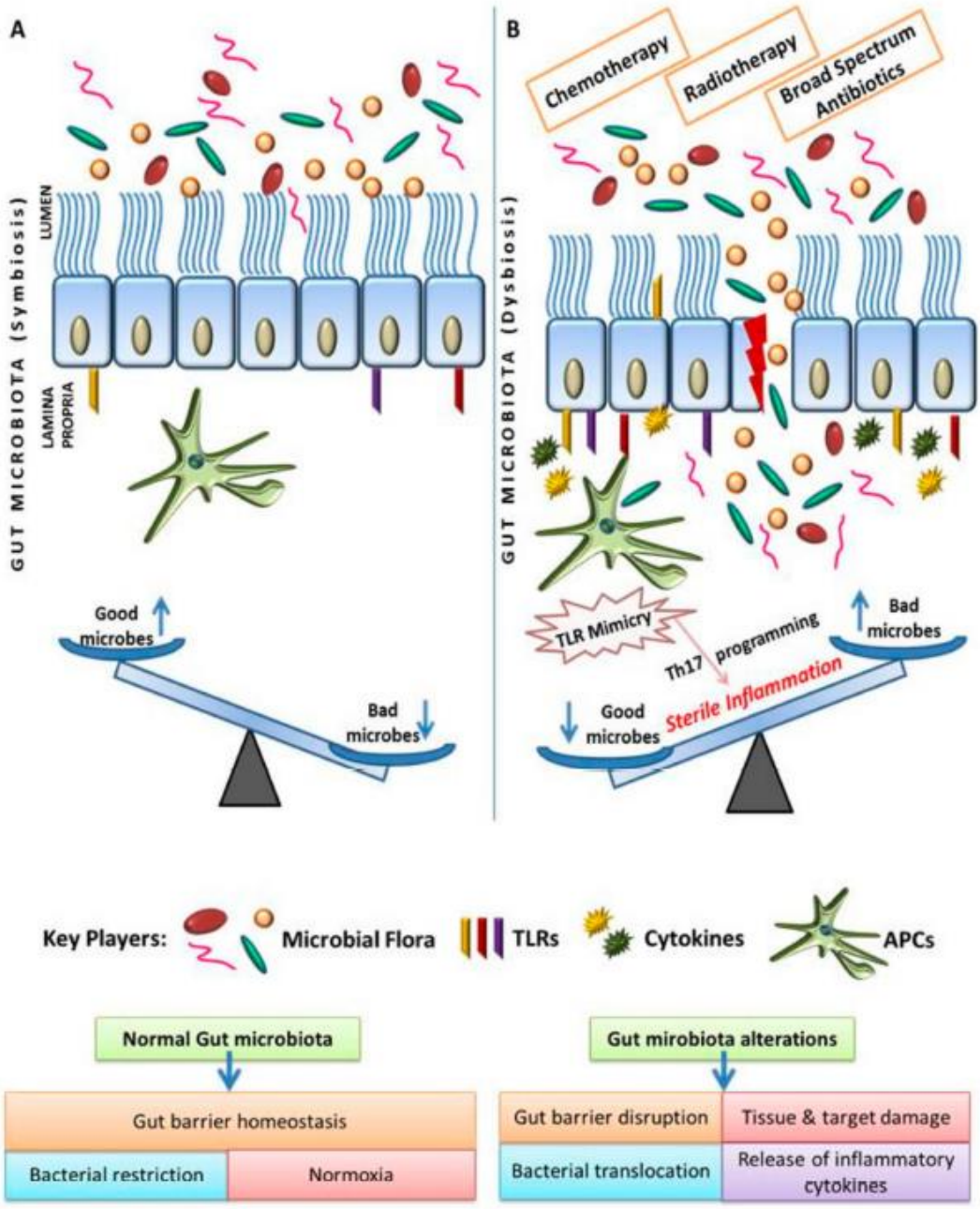

Fig. 1.7. Dysbiosis caused by medication and therapy [20].

1.2.2. Utilizing β-lactamase to protect microbiome

In 2016, M. Kaleko et al. reported a method to protect microbiome from antibiotics by oral administration of β-lactamases [34,35]. β-Lactamase is an enzyme that degrades

penicillin-type antibiotics. In this method, β-lactamase is orally administered before and after intravenous administration of the antibiotic and delivered to the large intestine. Thereby, a fraction of antibiotics reached the large intestine was degraded by β-lactamase to protect the intestinal flora. This method can protect the intestinal flora with a small amount of administration of the enzyme because of its high activity and specificity toward antibiotics. However, this promising approach is limited to penicillin-type antibiotics.

1.2.3. Activated carbon as antibiotics adsorbent

Activated carbon for medical use has been used to remove waste and drug overdose in patients with renal failure. In 2018, D. Gunzburg et al. reported a method to protect microbiome from antibiotics by using activated carbon [36,37]. In the method, activated carbon is orally administered before and after oral administration of antibiotics. The activated carbon reached to large intestine to trap antibiotics for protection of the gut flora. Finally, the activated carbon is excreted as stool (Fig. 1.8). However, activated carbon adsorbs hydrophobic substances nonspecifically which may result in adsorption of essential biological substances such as vitamins and fatty acid.

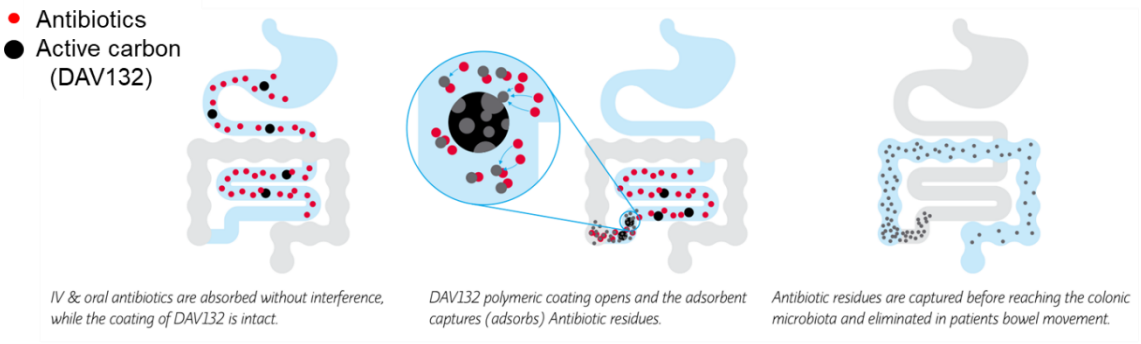

Fig. 1.8. Activated carbon for adsorbing residual antibiotics in large intestine.

1.3. Overview of this thesis

As mentioned above, the immunological homeostasis is disrupted by several reasons including antibiotic treatment. The disruption of immunological homeostasis results in diseases such as allergy and autoimmune diseases. To rebalance this situation, antigen-specific immunotolerance against allergen and auto-antigen should be induced.

Chapter 2 introduces vitamin-peptide conjugates that achieve co-delivery of immunomodulatory vitamins and antigen peptides to APC. Vitamins were selective modified on the peptide N-terminus that will not affect T cell recognition and MHC binding. Among the designed conjugated, retinoic acid-peptide conjugate showed anti-inflammatory effects, presented antigens on dendritic cells to activate T cells. The conjugates have the potential to treat allergy and auto-immune diseases by efficiently inducing antigen-specific immune tolerance.

In Chapter 3, I designed an antibiotic specific adsorbent to protect microbiome. Here I targeted vancomycin and utilizing a peptide ligand to capture vancomycin with relatively high affninity. The peptide ligands-loaded microparticles showed high selectivity and capacity for vancomycin, and exerted their effects in vivo to suppress dysbiosis and C. difficil infection associated with dysbiosis.

In Chapter 4, I summarized the conclusions of this paper. Then, I explained the prospects of my research conducted in this thesis.

1.4. References

[1] J. Ermann, C.G. Fathman, Autoimmune diseases: Genes, bugs and failed regulation, Nat. Immunol. 2 (2001) 759–761. https://doi.org/10.1038/ni0901-759.

[2] J. A. Hemler, E. J. Phillips, M. D, S. A. Mallal, M. B. B. S, P. L. Kendall, The Evolving Story of HLA and the Immunogenetics of Peanut Allergy, Ann Allergy Asthma Immunol. 115 (2015) 471-476. http://doi: 10. 1016/j.anai.2015.10.008

[3] K.M. Spach, F.E. Nashold, B.N. Dittel, C.E. Hayes, IL-10 Signaling Is Essential for 1,25-Dihydroxyvitamin D 3 -Mediated Inhibition of Experimental Autoimmune Encephalomyelitis , J. Immunol. 177 (2006) 6030–6037. https://doi.org/10.4049/jimmunol.177.9.6030.

[4] F.E. Nashold, K.A. Hoag, J. Goverman, C.E. Hayes, Rag-1-dependent cells are necessary for 1,25-dihydroxyvitamin D3 prevention of experimental autoimmune encephalomyelitis, J. Neuroimmunol. 119 (2001) 16–29. https://doi.org/10.1016/S0165-5728(01)00360-5.

[5] T.P. Wypych, B.J. Marsland, Antibiotics as Instigators of Microbial Dysbiosis: Implications for Asthma and Allergy, Trends Immunol. 39 (2018) 697–711. https://doi.org/10.1016/j.it.2018.02.008.

[6] L.S.K. Walker, EFIS Lecture: Understanding the CTLA-4 checkpoint in the maintenance of immune homeostasis, Immunol. Lett. 184 (2017) 43–50. https://doi.org/10.1016/j.imlet.2017.02.007.

[7] D. Saadoun, M. Rosenzwajg, D. Landau, J.C. Piette, D. Klatzmann, P. Cacoub, Restoration of peripheral immune homeostasis after rituximab in mixed cryoglobulinemia vasculitis, Blood. 111 (2008) 5334–5341. https://doi.org/10.1182/blood-2007-11-122713.

[8] H. Tsujimoto, P.A. Efron, T. Matsumoto, R.F. Ungaro, A. Abouhamze, S. Ono,

H. Mochizuki, L.L. Moldawer, Maturation of murine bone marrow-derived dendritic cells with poly(I:C) produces altered TLR-9 expression and response to CpG DNA, Immunol. Lett. 107 (2006) 155–162. https://doi.org/10.1016/j.imlet.2006.09.001.

[9] G. Hartmann, G.J. Weiner, A.M. Krieg, CpG DNA: A potent signal for growth, activation, and maturation of human dendritic cells, Proc. Natl. Acad. Sci. U. S. A. 96 (1999) 9305–9310. https://doi.org/10.1073/pnas.96.16.9305.

[10] S. Schlickeiser, S. Stanojlovic, C. Appelt, K. Vogt, S. Vogel, S. Haase, T. Ritter, H.-D. Volk, U. Pleyer, B. Sawitzki, Control of TNF-Induced Dendritic Cell Maturation by Hybrid-Type N -Glycans , J. Immunol. 186 (2011) 5201–5211. https://doi.org/10.4049/jimmunol.1003410.

[11] J.R. Gordon, Y. Ma, L. Churchman, S.A. Gordon, W. Dawicki, Regulatory dendritic cells for immunotherapy in immunologic diseases, Front. Immunol. 5 (2014) 1–19. https://doi.org/10.3389/fimmu.2014.00007.

[12] H. Hasegawa, T. Matsumoto, Mechanisms of tolerance induction by dendritic cells in vivo, Front. Immunol. 9 (2018). https://doi.org/10.3389/fimmu.2018.00350.

[13] J. Ring, Davos Declaration: Allergy as a global problem, Allergy Eur. J. Allergy Clin. Immunol. 67 (2012) 141–143. https://doi.org/10.1111/j.1398-9995.2011.02770.x.

[14] M. do C. Borralho, R.F. da Silva, A.S. Santana, R. de M. Caetano, Boas práticas da OMS para laboratórios de microbiologia farmacêutica de microbiologia farmacêutica, Série Rede Parf. 11 (2013) 1–37. https://doi.org/10.1016/j.jaut.2009.09.008.Recent.

[15] Japan intractable diseases information center, Transition data from 1975 to 2004, https://www.nanbyou.or.jp/entry/1356#p01

[16] M. Nishima, H. Odashima, K. Ota, N. Ota, K. Okazaki, M. Kanaya, N. Hisada, T. Kumamoto, T. Koga, N. Kobayashi, K. Satomi, Y. Shimada, M. Shimomura, M. Suda, I. Sunagawa, S.H. Osaka, Y. Nagata, T. Nakamura, K. Nishikawa, K. Hiraba, T. Fujino, T. Fujiwara, S. Honjo, T. Maeda, S. Matsumoto, T. Minami, Y. Miyazato, Prevalence Survey of Allergic Diseases in West Elementary School Children: Comparison in 1992, 2002, and 2012, Journal of Japanese Society of Pediatric Allergy, 27 (2013) 149-169, https://doi.org/10.3388/jspaci.27.149

[17] T.K. Kishimoto, R.A. Maldonado, Nanoparticles for the induction of antigen-specific immunological tolerance, Front. Immunol. 9 (2018). https://doi.org/10.3389/fimmu.2018.00230.

[18] R.A. Maldonado, R.A. LaMothe, J.D. Ferrari, A.H. Zhang, R.J. Rossi, P.N. Kolte, A.P. Griset, C. O'Neil, D.H. Altreuter, E. Browning, L. Johnston, O.C. Farokhzad, R. Langer, D.W. Scott, U.H. Von Andrian, T.K. Kishimoto, Polymeric synthetic nanoparticles for the induction of antigen-specific immunological tolerance, Proc. Natl. Acad. Sci. U. S. A. 112 (2015) E156–E165. https://doi.org/10.1073/pnas.1408686111.

[19] R.E. Ley, D.A. Peterson, J.I. Gordon, Ecological and evolutionary forces shaping microbial diversity in the human intestine, Cell. 124 (2006) 837–848. https://doi.org/10.1016/j.cell.2006.02.017.

[20] C. Bruhn, Wohngemeinschaft Haut, Dtsch. Apotheker Zeitung. 157 (2017) e1002. https://doi.org/10.1371/journal.pbio.1002533.

[21] P.J. Turnbaugh, R.E. Ley, M. Hamady, C.M. Fraser-Liggett, R. Knight, J.I. Gordon, The Human Microbiome Project, Nature. 449 (2007) 804–810. https://doi.org/10.1038/nature06244.

[22] D. Toor, M.K. Wasson, P. Kumar, G. Karthikeyan, N.K. Kaushik, C. Goel, S. Singh, A. Kumar, H. Prakash, Dysbiosis disrupts gut immune homeostasis and

promotes gastric diseases, Int. J. Mol. Sci. 20 (2019) 1–14. https://doi.org/10.3390/ijms20102432.

[23] M. Yousaf, Inayatullah, A.R. Khan, N. Ahmad, S. Ali, The presentation pattern of otitis media with effusion, J. Med. Sci. 17 (2009) 53–55. https://doi.org/10.1126/scitranslmed.3009759.The.

[24] E.Y. Hsiao, S.W. McBride, S. Hsien, G. Sharon, E.R. Hyde, T. McCue, J.A. Codelli, J. Chow, S.E. Reisman, J.F. Petrosino, P.H. Patterson, S.K. Mazmanian, Microbiota modulate behavioral and physiological abnormalities associated with neurodevelopmental disorders, Cell. 155 (2013) 1451–1463. https://doi.org/10.1016/j.cell.2013.11.024.

[25] Q. Zhao, C.O. Elson, Adaptive immune education by gut microbiota antigens, Immunology. 154 (2018) 28–37. https://doi.org/10.1111/imm.12896.

[26] T. Tanoue, K. Atarashi, K. Honda, Development and maintenance of intestinal regulatory T cells, Nat. Rev. Immunol. 16 (2016) 295–309. https://doi.org/10.1038/nri.2016.36.

[27] K. Atarashi, T. Tanoue, K. Oshima, W. Suda, Y. Nagano, H. Nishikawa, S. Fukuda, T. Saito, S. Narushima, K. Hase, S. Kim, J. V. Fritz, P. Wilmes, S. Ueha, K. Matsushima, H. Ohno, B. Olle, S. Sakaguchi, T. Taniguchi, H. Morita, M. Hattori, K. Honda, Treg induction by a rationally selected mixture of Clostridia strains from the human microbiota, Nature. 500 (2013) 232–236. https://doi.org/10.1038/nature12331.

[28] S.K. Lathrop, S.M. Bloom, S.M. Rao, K. Nutsch, C.W. Lio, N. Santacruz, D.A. Peterson, T.S. Stappenbeck, C.S. Hsieh, Peripheral education of the immune system by colonic commensal microbiota, Nature. 478 (2011) 250–254. https://doi.org/10.1038/nature10434.

[29] E. Blacher, M. Levy, E. Tatirovsky, E. Elinav, Microbiome-Modulated

Metabolites at the Interface of Host Immunity, J. Immunol. 198 (2017) 572–580. https://doi.org/10.4049/jimmunol.1601247.

[30] L.E. Papanicolas, D.L. Gordon, S.L. Wesselingh, G.B. Rogers, Not Just Antibiotics: Is Cancer Chemotherapy Driving Antimicrobial Resistance?, Trends Microbiol. 26 (2018) 393–400. https://doi.org/10.1016/j.tim.2017.10.009.

[31] Y. and T.H. Belkaid, Role of the Microbiota in Immunity and inflammation Yasmine, Cell. 157 (2015) 121–141. https://doi.org/10.1016/j.cell.2014.03.011.Role.

[32] S.L. Russell, M.J. Gold, M. Hartmann, B.P. Willing, L. Thorson, M. Wlodarska, N. Gill, M.R. Blanchet, W.W. Mohn, K.M. McNagny, B.B. Finlay, Early life antibiotic-driven changes in microbiota enhance susceptibility to allergic asthma, EMBO Rep. 13 (2012) 440–447. https://doi.org/10.1038/embor.2012.32.

[33] S.L. Russell, M.J. Gold, B.P. Willing, L. Thorson, K.M. McNagny, B.B. Finlay, Perinatal antibiotic treatment affects murine microbiota, immune responses and allergic asthma, Gut Microbes. 4 (2013) 158–164. https://doi.org/10.4161/gmic.23567.

[34] M. Kaleko, J.A. Bristol, S. Hubert, T. Parsley, G. Widmer, S. Tzipori, P. Subramanian, N. Hasan, P. Koski, J. Kokai-Kun, J. Sliman, A. Jones, S. Connelly, Development of SYN-004, an oral beta-lactamase treatment to protect the gut microbiome from antibiotic-mediated damage and prevent Clostridium difficile infection, Anaerobe. 41 (2016) 58–67. https://doi.org/10.1016/j.anaerobe.2016.05.015.

[35] T.O. Syn-, J.F. Kokai-kun, T. Roberts, O. Coughlin, E. Sicard, M. Rufiange, R. Fedorak, C. Carter, M.H. Adams, J. Longstreth, H. Whalen, crossm Clinical Studies, 61 (2017) 14–16.

[36] J. De Gunzburg, A. Ghozlane, A. Ducher, E. Le Chatelier, X. Duval, E. Ruppé,

L. Armand-Lefevre, F. Sablier-Gallis, C. Burdet, L. Alavoine, E. Chachaty, V. Augustin, M. Varastet, F. Levenez, S. Kennedy, N. Pons, F. Mentré, A. Andremont, Protection of the human gut microbiome from antibiotics, J. Infect. Dis. 217 (2018) 628–636. https://doi.org/10.1093/infdis/jix604.

[37] C. Burdet, S. Sayah-Jeanne, T.T. Nguyen, C. Miossec, N. Saint-Lu, M. Pulse, W. Weiss, A. Andremont, F. Mentré, J. De Gunzburg, Protection of hamsters from mortality by reducing fecal moxifloxacin concentration with DAV131A in a model of moxifloxacin-induced Clostridium difficile colitis, Antimicrob. Agents Chemother. 61 (2017) 1–9. https://doi.org/10.1128/AAC.00543-17.

CHAPTER 2

Development of vitamin-peptide conjugate for induction of antigen-specific immunotolerance

2.1. Introduction

Recently, patients with allergic and autoimmune diseases have been rapidly increasing worldwide [1,2]. To treat these diseases, antigen-specific immunotolerance toward allergens and auto-antigens should be induced [3]. The immunotolerance is induced by dendritic cells (DCs) with tolerogenic phenotype which are called tolerogenic DCs (tDCs). tDCs induce an anergetic response to helper T cells as well as differentiate naïve T cells to regulatory T cells (T_{reg} cells), which are executer of antigen-specific immunotolerance. T_{reg} cells expressing CD4 ($CD4^+$ T_{reg}) compete with helper T cells to induce immunotolerance, while T_{reg} cells expressing CD8 ($CD8^+$ T_{reg}) contribute to induce immunotolerance by several pathways such as secretion of cytokines [4–7].

It has been reported that induction of tDC is facilitated by small molecules such as vitamins and rapamycin [8,9]. For efficient induction of antigen-specific immunotolerance, nanoparticle formulations containing both antigens and tDC-inducing molecules have been reported [10]. We also reported previously nanoparticles of allergen proteins incorporated with all-*trans* retinoic acid (ATRA) which is one of the representative tDC-inducing molecules [11].

Here we proposed peptide-vitamin conjugates to achieve co-delivery of vitamins and antigen peptide to DCs for effective induction of tDCs and T_{reg} cells (Fig.2.1). We chose ATRA and vitamin D3 (vD3) [12–15] as inducing molecules of tDC. The

conjugates are taken up by DC and release antigen peptides and vitamins from the conjugates by lysosomal peptidases. Antigen peptide is presented on the surface of DC through intracellular process, and vitamins bind to corresponding nuclear receptors to induce differentiation of tDC thereby facilitating the T_{reg} induction. The antigen peptide and vitamin were connected with three arginine residues (Fig. 2.2) which is a cleavable sequence of an endosomal peptidases such as cathepsin B [16,17]. The three-arginine linker will enhance the solubility of the conjugates containing hydrophobic vitamins. We established general scheme to synthesize the conjugates and investigated whether the scheme shown in Fig. 2.1 was conducted in vitro.

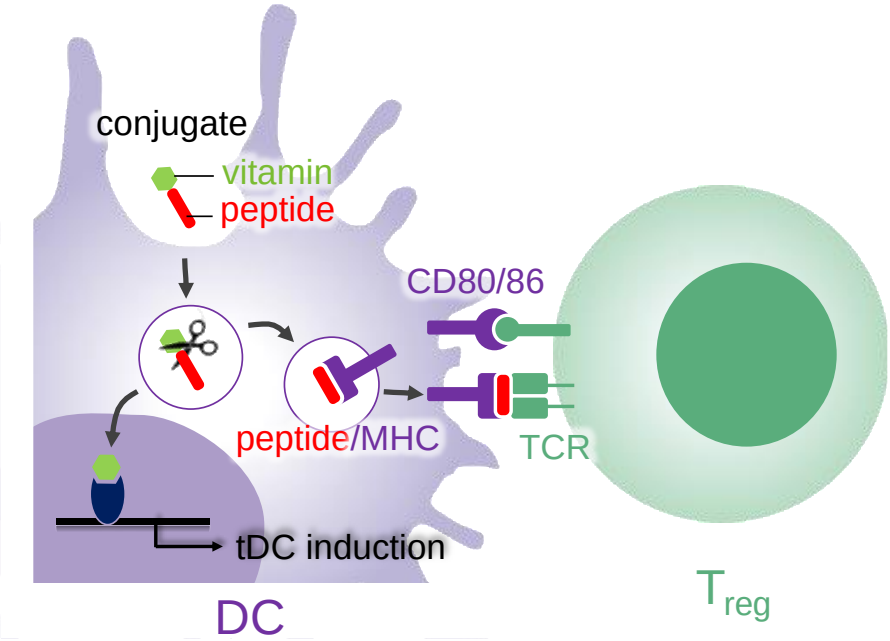

Fig. 2.1. Schematic representation of induction of tDC and T_{reg} by peptide-vitamin conjugates. Conjugate taken up DC releases an antigen peptide and a vitamin by lysosomal peptidases. The resulting vitamin bound to a corresponding nuclear receptor to differentiate DC to tDC. The resulting peptide is presented on a major histocompatibility

complex (MHC) protein to stimulate a T cell receptor (TCR) thereby inducing T_{reg} cell.

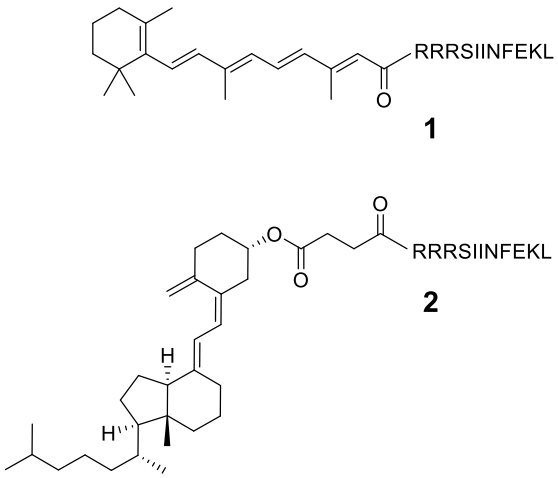

Fig. 2.2. Structure of peptide-ATRA (**1**) and peptide-vD3 conjugates (**2**). Three arginine residues on N-terminus are linker between antigen peptide (SIINFEKL) and vitamins.

2.2. Materials and Methods

2.2.1. Synthesis of lysine residue-protected peptide

Peptide was synthesized on Nova syn TGA resin at a 0.2-mmol scale by Fmoc solid-phase peptide synthesis. 1-Hydroxy-1H-benzotriazole hydrate and O-(1H-benzotriazol-1-yl)-N,N,N',N'-tetramethyluronium hexafluorophosphate were used as the condensing agents. For the N-terminal amino acid, tert-butoxycarbonyl (Boc)-protected one was used. After the completion of elongation of peptide main chain, 4-methyltrityl (Mtt) protection group of lysine residue was removed by 10% trifluoroacetic acid (TFA) / dichloromethane (DCM). Then, N-(9-fluorenylmethoxycarbonyloxy) (Fmoc) group was modified on the lysine residue by using Fmoc succinimide (Fmoc-OSu). The peptide was then cleaved

from the resin by treatment with TFA containing 2.5% (v/v), triisopropyl silane (TIS) and 2.5% (v/v) water, and purified by reversed-phase high-performance liquid chromatography (HPLC) (Hitachi Chromatomaster, Tokyo, Japan) on an Altantis dC18 OBD column (19x100 mm) (waters corporation, MA, USA) using a mobile phase consisting of acetonitrile/0.1%TFA and H_2O/0.1%TFA. The obtained lysine residue-protected peptide was identified by a matrix-assisted laser desorption ionization time-of-flight (MALDI-TOF) mass spectrometer (Bruker Daltonics, Billerica, MA, USA).

2.2.2. Synthesis of conjugate 1 and 2

N-Hydroxysuccinimide ester (NHS) of vitamins (ATRA-NHS, vD3-succinic acid-NHS) were synthesized according to literatures [18,19]. The lysine residue-protected peptide (1 mM) and vitamin-NHS (10 mM) were dissolved in dimethylformamide (DMF). N,N-Diisopropylethylamine (DIEA) (10 mM) was added to the solution and reacted at room temperature overnight under nitrogen. After the reaction, Fmoc group of lysine residue was removed with 20% piperidine (PPD)/DMF and the resulting conjugate was purified by reversed-phase HPLC. The obtained conjugates were identified by a MALDI-TOF mass spectrometer (Fig.2.3).

2.2.3. Cell line and culture

RAW 264.7 macrophages transfected with secreted alkaline phosphatase (SEAP) as a reporter gene under the transcriptional control of a nuclear factor-kappa B (NF-κB) response element (Novusbio) were maintained in Dulbecco's Modified Eagle's Medium (DMEM) supplemented with 10% (v/v) fetal bovine serum (FBS), 100 U/mL penicillin, 100 μg/mL streptomycin, 0.25 μg/mL amphotericin B (Invitrogen, grand island, NY, USA) and 500 μg/mL G418 (only for the RAW 264.7 macrophages transfected with SEAP). DC2.4 cells were kindly provided by Dr. Kenneth Rock (University of

Massachusetts Medical Center, Worcester, MA, USA) [20]. The cells were maintained in Roswell Park Memorial Institute media (RPMI1640) medium supplemented with 10% (v/v) FBS, 100 U/mL penicillin, 100 µg/mL streptomycin, and 0.25 µg/mL amphotericin B. CD8OVA1.3 T hybridoma cell were kindly provided by Dr. Clifford V. Harding (Case Western Reserve University, Cleveland, OH) [21]. The cells were maintained in RPMI1640 medium supplemented with 10% (v/v) FBS, 100 U/mL penicillin, 100 µg/mL streptomycin, 0.25 µg/mL amphotericin B, and 2-mercaptoethanol. Cells were incubated in a humidified atmosphere containing 5% CO2 at 37°C.

2.2.4. Cell viability

DC2.4 cells (2×10^5 cell/well) were seeded in 48-well plates, grown for 24 h then exposed for 24 h at 37°C to conjugate 1 or 2 in culture media. Propidium iodide (PI) was added a few minutes before analyzing the cells by using a Tali® image-based cytometer (Thermo Fisher Scientific). Excitation and emission wavelengths were 488 and 620 nm respectively.

2.2.5. Alkaline phosphatase assay

RAW 264.7 macrophages transfected with SEAP (4×104 cells/well) were cultured in a 48-well plate with complete DMEM. After incubation overnight, the medium was replaced with complete DMEM containing conjugate 1 or 2. The supernatant were discarded and the cells were treated with lipopolysaccharide (LPS) (Sigma-Aldrich) (10 ng/mL) for 24h. After incubation, the supernatants were mixed with an equal volume of alkaline phosphatase substrate (1 mg/mL p-nitrophenylphosphate) and incubated at room temperature for 1.5 h and then 3 N NaOH was added to stop the reaction. The optical density of the solution was measured at 405 nm with a microplate reader (Wallac ARVO.SX 1420 Multilabel counter).

2.2.6. Quantitative real-time-PCR assays (qRT-PCR)

DC2.4 cells (2×10^5 cell/well) were plated in 24-well plates with RPMI1640. After incubation overnight, the medium was replaced with complete RPMI1640 containing conjugate 1. After 24 h, LPS (final conc. 10 ng/mL) was added and the cells were incubated for 24 h. The total RNA from the cells was prepared using isoPlus reagent (Takara). The samples were reverse-transcribed using the SuperScript III First-Strand Synthesis System (Invitrogen) and the synthesized cDNA was used as a template in qPCR experiments performed with a LightCycler 1.5 (Roche Diagnostics, Germany) and analyzed with LightCycler Manager software 3.5 (Roche Diagnostics, Germany). The relative expression level was calculated by the ΔΔCt method using Gapdh as a reference gene. All primers were purchased from Takara-Clontech Laboratories (Japan) (Table 2.1).

2.2.7. Flow cytometry

MHC-II, CD80, and CD86 expression levels were measured after incubating DC2.4 cells with conjugate 1 or ATRA (1 μM) for overnight. Cells were washed with DPBS and re-suspended in FACS buffer (2 wt% BSA containing PBS) and stained with APC-anti mouse CD80 mAb (BioLegend), APC-anti mouse CD86 mAb (BioLegend) and PE-anti mouse MHC-II mAb (BioLegend) by incubating in the dark at 4 °C for 15 min. Cells were washed with FACS buffer and analyzed by a cytoflex flow cytometer (Backman coulter).

2.2.8. Antigen presentation assay

DC2.4 cells (2×10^5 cell/well) were plated in 24-well plates with RPMI1640 and incubated 24 h. Conjugate 1 or free peptide (0.1 μM) were added to each well and incubated for 6 h. After discarding supernatant, suspension of CD8OVA1.3 T cells (2×10^5 cell/well) was

added in each well, then the plates were centrifuged at 450 g to initiate contact between the cells. The cells were incubated together at 37 °C. Then, the response of CD8OVA1.3 T cells was determined by measuring IL-2 levels in the supernatants with enzyme-linked immunosorbent assay (ELISA) (mouse IL-2, Invitrogen).

2.3. Results and Discussion

2.3.1. Synthesis of vitamin-peptide conjugate

Here we used peptide sequence (SIINFEKL) derived from ovalbumin 257-264, which is widely used as a model antigen and can be presented on an MHC class I. We designed conjugate 1 and 2 with a vitamin on N-terminus of the peptide through a linker of three arginine residues (Fig. 2.2). We failed to synthesize the conjugates on a resin because ATRA and vD3 did not tolerate to strongly acidic condition which was used for cleavage of peptide from a resin. Thus we decided to modify the vitamins on the peptide in solution phase and established general scheme to synthesize conjugates which is applicable to peptides containing lysine residue (Scheme 2.1). After the synthesis of the peptide with N-terminus Boc protection on the resin, the protecting group of the lysine residue was converted from Mtt to acid-tolerable Fmoc, then the peptide was cleaved from the resin and purified. To the peptide with a protected lysine, NHS ester of ATRA was modified on N-terminus and finally Fmoc group was removed by weakly basic condition to which ATRA was tolerable. Conjugate 2 with vD3 was prepared by the same scheme with conjugate 1, except for NHS ester of succinated vD3 was used for conjugation.

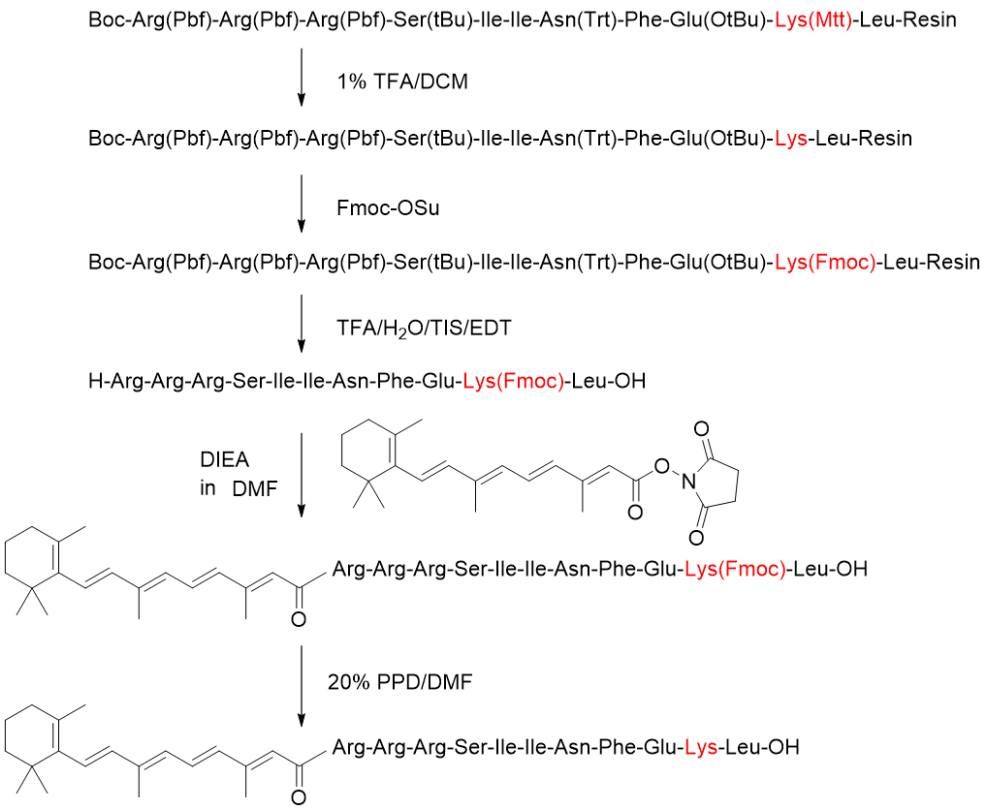

Scheme 2.1. Synthesis of 1

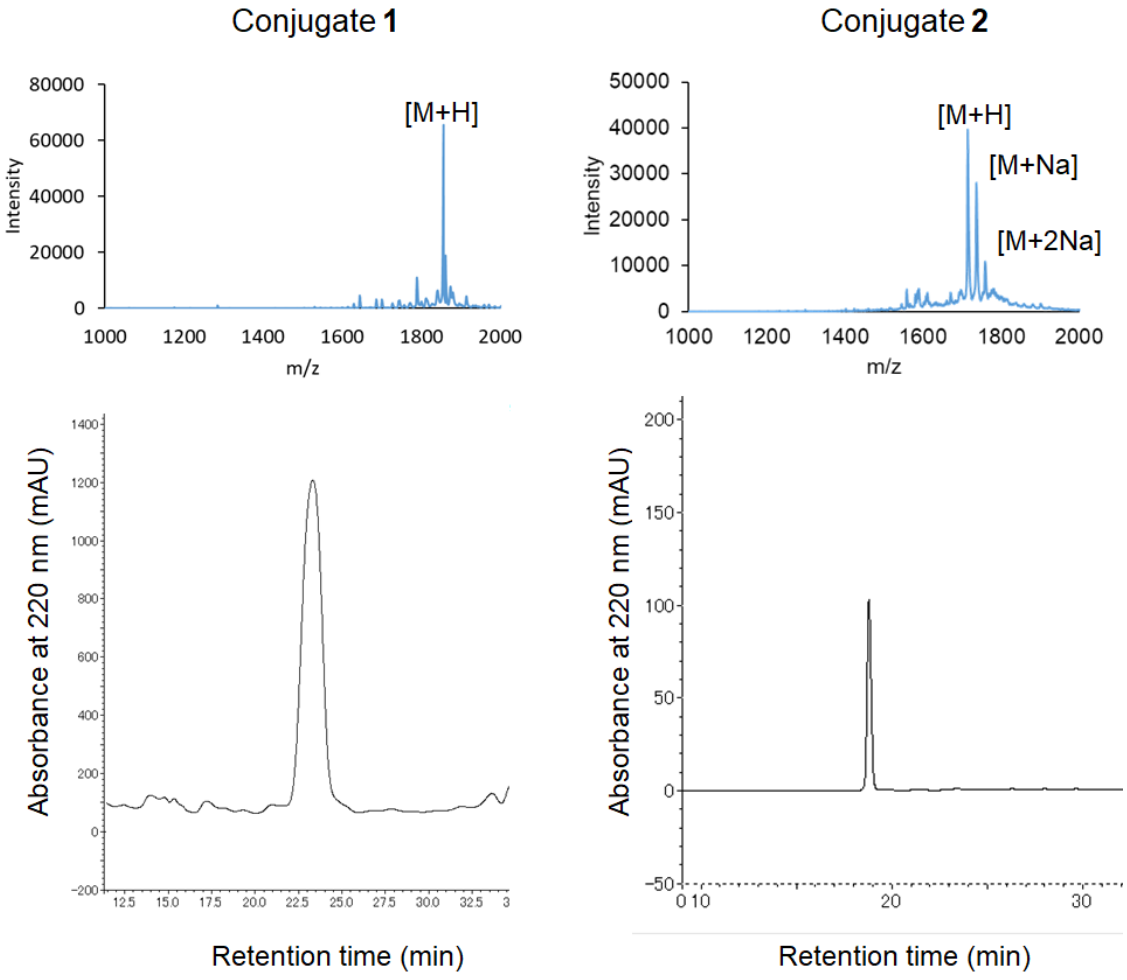

Fig. 2.3. MALDI-TOF mass spectra and chromatogram of conjugate **1** and **2**.

2.3.2. Cytotoxicity of conjugates

We compared cytotoxicity of the conjugates with free vitamins on a mouse cell line derived from DC (DC2.4). The cell viability was evaluated by PI staining after 24h. As shown in Fig.2.4, cytotoxicity of free vitamins and the corresponding conjugates was almost same. ATRA and conjugate 1 did not show significant cytotoxicity up to the examined concentration range. vD3 and conjugate 2 showed significant toxicity at 100 μM. The same cytotoxic profiles of free vitamins and the corresponding conjugates indicates that the conjugates which have amphiphilic nature due to the hydrophilic peptide

and hydrophobic vitamins does not perturb cell membrane to induce cytotoxicity.

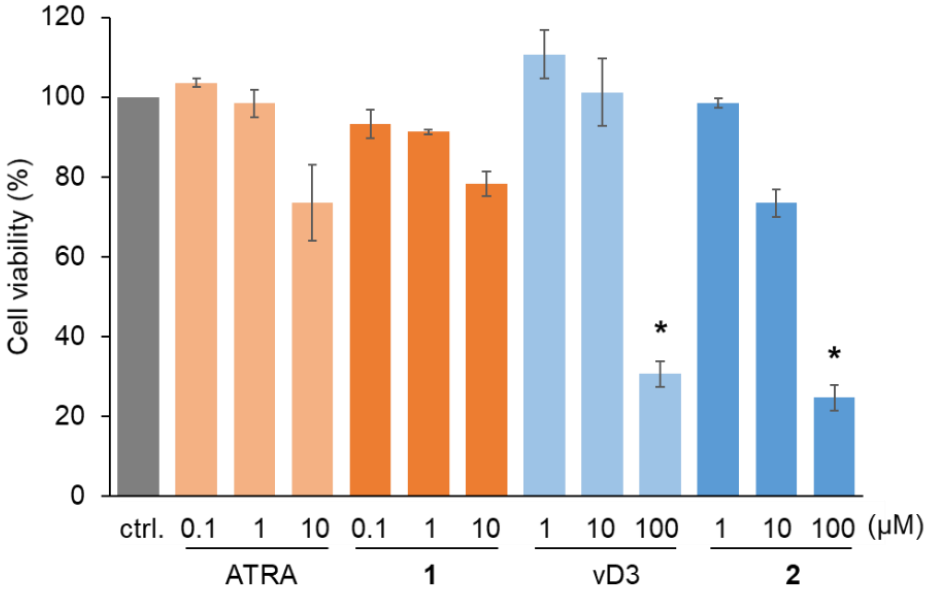

Fig. 2.4. Viability of DC2.4 cells after treatment with conjugates or free vitamins for 24 h. Dead cells were stained with PI and counted using image cytometer. Data represent the mean ± SD (n = 3). * $P < 0.05$, as compared with non-treated group (ctrl).

2.3.3. Alkaline phosphatase assay

We investigated release of vitamins from the conjugates using mouse macrophage cell line. Here we used RAW 264.7 macrophage transfected with SEAP as a reporter gene induced by the NF-κB transcription factor. If the conjugate shows anti-inflammatory response, free ATRA or vD3 is released from the conjugate. The cells were incubated with the conjugate or free vitamins then stimulated with LPS. As shown in Fig.2.5, free ATRA and vD3 showed suppression of macrophage activation at concentrations of 0.1 and 10 μM, respectively. The requirement of free vD3 for higher concentration will result from the requirement of conversion of vD3 to its active form by intracellular enzymes for binding to a nuclear receptor [22]. As for the conjugates, vD3 conjugate **2** did not show

suppressive effect, while ATRA conjugate **1** showed suppressive effect from the concentration of 1 μM. Although conjugate **1** required higher concentrations than free ATRA, the suppressive effect of **1** showed the release of free ATRA from **1**. The requirement of higher concentration of **1** than free ATRA may result from lower efficacy of cellular uptake as well as requirement of enzymatic process to release free ATRA.

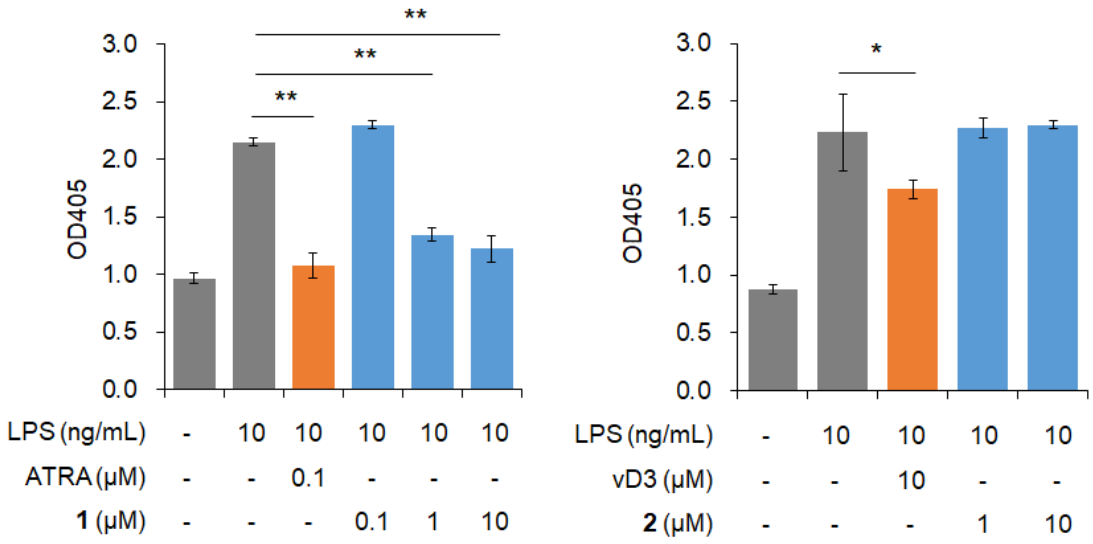

Fig. 2.5. Suppressive effect of conjugates and free vitamins on the LPS-induced NF-κB activation in RAW264.7 macrophages. After 24 h from the addition of each conjugate or free vitamin to macrophages, LPS (10 ng/mL) was added to the medium and incubated for a further 24 h. Absorbance resulting from substrate reacted with SEAP in supernatant was measured at 405 nm. Data are the mean ± SD (n = 3). *P < 0.05, **P < 0.01.

2.3.4. Suppression of LPS-induced inflammatory response of DC by ATRA conjugate

Next, we investigated the effects of ATRA conjugate 1 on the gene expression of cytokines in DC2.4 cells stimulated with LPS. As shown in Fig.2.6, both free ATRA and

conjugate 1 suppressed the expression of inflammatory cytokines, IL-6 and TNF-α. However, the expression of anti-inflammatory cytokines (IL-10, TGF-β) was not affected by both ATRA and conjugate 1. These results were consistent with previous reports about the response of bone marrow derived DCs to ATRA [23–25]. Therefore, free ATRA would be released from 1 in DC2.4 cells to induce suppressive effect against LPS-induced inflammatory response.

Table 2.1. Primer sequences used for RT-qPCR.

Transcript	**Forward primer**	**Reverse primer**
Il6	5'-CCACTTCACAAGTCGGAGGCTTA-3'	5'-CCAGTTTGGTAGCATCCATCATTTC-3'
Tnf	5'-ACCCTCACACTCAGATCATCTTC-3'	5'-TGGTGGTTTGCTACGACGT-3'
Gapdh	5'-CCCAGCAAGGACACTGAGCAAG-3'	5'-GGTCTGGGATGGAAATTGTGAGGG-3'
Tgf	5'-GTGTGGAGCAACATGTGGAACTCTA-3'	5'-CGCTGAATCGAAAGCCCTGTA-3'
Il-10	5'-TGCCTTCAGCCAGGTGAAGACTTTC-3'	5'-CTTGATTTCTGGGCCATGCTTCTCTG-3'

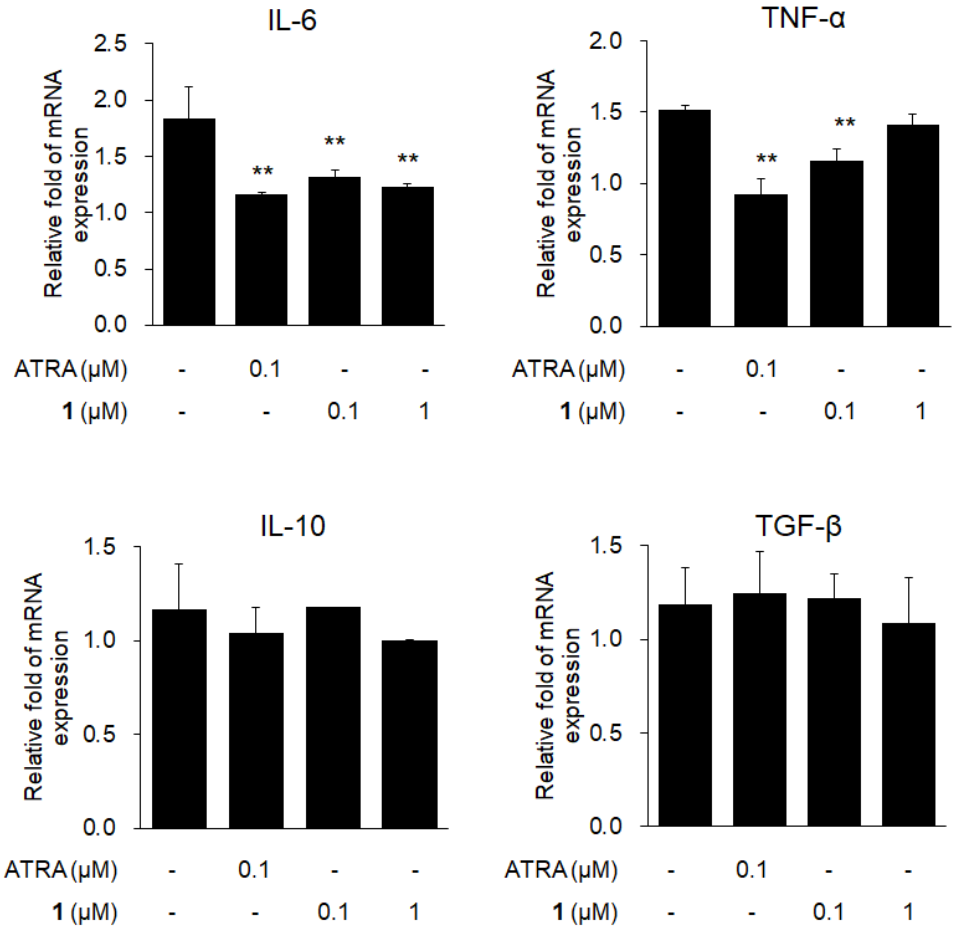

Fig. 2.6. Suppressive effect of conjugates on the gene expression of cytokines in DC2.4 cells. After addition of conjugates to dendritic cells for 24 h, LPS (10 ng/mL) was added and incubated for a further 24 h. And gene expression was evaluated by qRT-PCR. Data are the mean ± SD ($n = 3$). $^{*}P < 0.05$, $^{**}P < 0.01$, $^{***}P < 0.001$.

2.3.5. Expression of ligand on surface of DC2.4 cells

We compared effect of conjugate 1 with free ATRA on the ligand expression of DC2.4 cells. As shown in Fig.2.7, conjugate 1 showed similar effect on the ligand expression;

reduction of MHC class II and no effect on costimulatory ligands CD80 and CD86. The effect of ATRA on the ligands expression of DC is controversial because it seems to differ up to the experimental setup. However, the reduction of MHC class II has been observed for many reports [26–29], and this phenotype is typical one in tDC [30].

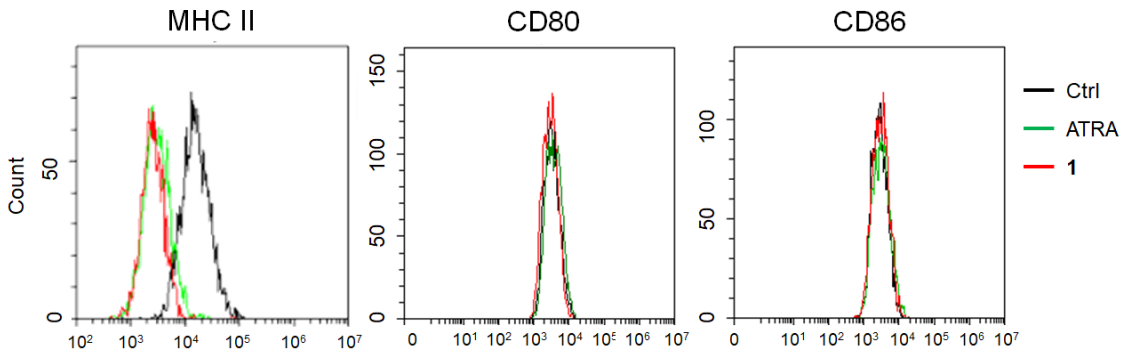

Fig. 2.7 Comparison of effect of conjugate **1** with free ATRA on the ligand expression of DC2.4 cells. After 24 h from the addition of conjugate or ATRA (0.1 μM) to DC2.4 cells, expression of each protein was analyzed by flow cytometry.

2.3.6. Conjugate induction of antigen-specific immune responses

Presentation of peptide from conjugate **1** on DC2.4 was evaluated by stimulation of $CD8^+$ T cell hybridoma. DC2.4 cells were pulsed with conjugate **1** and to this was added CD8OVA 1.3 T cell hybridoma (which can be activated by OVA257-264/K^b complex) [21]. Stimulation of the T cell hybridoma by DC2.4 was evaluated by secretion of IL-2. As shown in Fig.2.8, conjugate **1** induced production of IL-2 though the induction efficacy was lower than free peptide (SIIFEKL). This result indicated that peptide was cleaved from the conjugate in DC2.4 cells and presented on the cell surface.

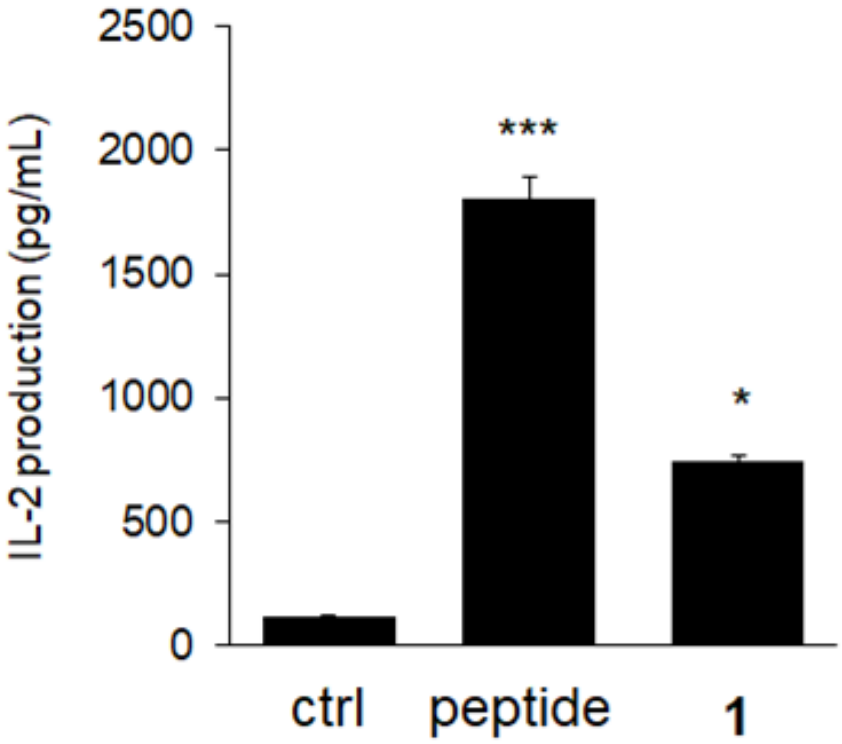

Fig. 2.8. Evaluation of antigen presentation on DC2.4 from conjugate **1** to $CD8^+$ T cell hybridoma. DC2.4 cells were pulsed with conjugate **1** or free peptide (0.1 μM) for 6 h and then co-cultured with CD8OVA1.3 T cells for 18 h. IL-2 production in supernatant was measured by ELISA. Data are the mean ±SD (n = 3). *P < 0.05, ***P < 0.001, as compared with ctrl group (non-treated DC + hybridoma).

2.4. Conclusions

We established synthetic scheme of peptide-vitamin conjugates. ATRA conjugate was edited in both macrophage and DCs to show the anti-inflammatory effect derived from ATRA. ATRA conjugate was also edited in DCs to present peptide/MHC class I complex to stimulate T cell hybridoma. The conjugates developed here will be useful to facilitate the induction of antigen-specific immunotolerance for the therapy of allergic and autoimmune diseases.

2.5. References

[1] E.N. Grant, M. Robin Wagner, K.B. Weiss, Observations on emerging patterns of asthma in our society, J. Allergy Clin. Immunol. 104 (1999) 1–9. https://doi.org/10.1016/S0091-6749(99)70268-X.

[2] W.-J. Song, M.-G. Kang, Y.-S. Chang, S.-H. Cho, Epidemiology of adult asthma in Asia: toward a better understanding, Asia Pac. Allergy. 4 (2014) 75. https://doi.org/10.5415/apallergy.2014.4.2.75.

[3] M. Miyara, K. Wing, S. Sakaguchi, Therapeutic approaches to allergy and autoimmunity based on FoxP3+ regulatory T-cell activation and expansion, J. Allergy Clin. Immunol. 123 (2009) 749–755. https://doi.org/10.1016/j.jaci.2009.03.001.

[4] A. Schmidt, N. Oberle, P.H. Krammer, Molecular mechanisms oftreg-mediatedt cell suppression, Front. Immunol. 3 (2012) 1–20. https://doi.org/10.3389/fimmu.2012.00051.

[5] M. Caridade, L. Graca, R.M. Ribeiro, Mechanisms underlying CD4+ Treg immune regulation in the adult: From experiments to models, Front. Immunol. 4 (2013) 1–9. https://doi.org/10.3389/fimmu.2013.00378.

[6] Y. Yu, X. Ma, R. Gong, J. Zhu, L. Wei, J. Yao, Recent advances in CD8+ regulatory t cell research (Review), Oncol. Lett. 15 (2018) 8187–8194. https://doi.org/10.3892/ol.2018.8378.

[7] S. Bézie, I. Anegon, C. Guillonneau, Advances on CD8+ Treg Cells and Their Potential in Transplantation, Transplantation. 102 (2018) 1467–1478. https://doi.org/10.1097/TP.0000000000002258.

[8] A. Schmidt, M. Eriksson, M.M. Shang, H. Weyd, J. Tegnér, Comparative analysis of protocols to induce human CD4+Foxp3+ regulatory T cells by combinations of IL-2, TGF-beta, retinoic acid, rapamycin and butyrate, PLoS One. 11 (2016) 1–31.

https://doi.org/10.1371/journal.pone.0148474.

[9] J.R. Gordon, Y. Ma, L. Churchman, S.A. Gordon, W. Dawicki, Regulatory dendritic cells for immunotherapy in immunologic diseases, Front. Immunol. 5 (2014) 1–19. https://doi.org/10.3389/fimmu.2014.00007.

[10] R.A. Maldonado, R.A. LaMothe, J.D. Ferrari, A.H. Zhang, R.J. Rossi, P.N. Kolte, A.P. Griset, C. O'Neil, D.H. Altreuter, E. Browning, L. Johnston, O.C. Farokhzad, R. Langer, D.W. Scott, U.H. Von Andrian, T.K. Kishimoto, Polymeric synthetic nanoparticles for the induction of antigen-specific immunological tolerance, Proc. Natl. Acad. Sci. U. S. A. 112 (2015) E156–E165. https://doi.org/10.1073/pnas.1408686111.

[11] K. Zai, K. Yuzuriha, A. Kishimura, T. Mori, Y. Katayama, Preparation of complexes between ovalbumin nanoparticles and retinoic acid for efficient induction of Tolerogenic dendritic cells, Anal. Sci. 34 (2018) 1243–1248. https://doi.org/10.2116/analsci.18P252.

[12] T. Nikolic, B.O. Roep, Regulatory multitasking of tolerogenic dendritic cells - lessons taken from vitamin D3-treated tolerogenic dendritic cells, Front. Immunol. 4 (2013) 1–13. https://doi.org/10.3389/fimmu.2013.00113.

[13] G.B. Ferreira, C.A. Gysemans, J. Demengeot, J.P.M.C.M. da Cunha, A.-S. Vanherwegen, L. Overbergh, T.L. Van Belle, F. Pauwels, A. Verstuyf, H. Korf, C. Mathieu, 1,25-Dihydroxyvitamin D 3 Promotes Tolerogenic Dendritic Cells with Functional Migratory Properties in NOD Mice , J. Immunol. 192 (2014) 4210–4220. https://doi.org/10.4049/jimmunol.1302350.

[14] S. Agrawal, S. Ganguly, A. Tran, P. Sundaram, A. Agrawal, Retinoic acid treated human dendritic cells induce T regulatory cells via the expression of CD141 and GARP which is impaired with age, Aging (Albany. NY). 8 (2016) 1223–1235. https://doi.org/10.18632/aging.100973.

[15] G. Bakdash, L.T.C. Vogelpoel, T.M.M. Van Capel, M.L. Kapsenberg, E.C. De Jong, Retinoic acid primes human dendritic cells to induce gut-homing, IL-10-producing regulatory T cells, Mucosal Immunol. 8 (2015) 265–278. https://doi.org/10.1038/mi.2014.64.

[16] S.S. Cotrin, L. Puzer, W.A. De Souza Judice, L. Juliano, A.K. Carmona, M.A. Juliano, Positional-scanning combinatorial libraries of fluorescence resonance energy transfer peptides to define substrate specificity of carboxydipeptidases: Assays with human cathepsin B, Anal. Biochem. 335 (2004) 244–252. https://doi.org/10.1016/j.ab.2004.09.012.

[17] G. Hook, J.S. Jacobsen, K. Grabstein, M. Kindy, V. Hook, Cathepsin B is a new drug target for traumatic brain injury therapeutics: Evidence for E64d as a promising lead drug candidate, Front. Neurol. 6 (2015) 1–27. https://doi.org/10.3389/fneur.2015.00178.

[18] G. Magoulas, D. Papaioannou, E. Papadimou, D. Drainas, Preparation of spermine conjugates with acidic retinoids with potent ribonuclease P inhibitory activity, Eur. J. Med. Chem. 44 (2009) 2689–2695. https://doi.org/10.1016/j.ejmech.2009.01.001.

[19] S. Patil, S. Gawali, S. Patil, S. Basu, Synthesis, characterization and in vitro evaluation of novel vitamin D3 nanoparticles as a versatile platform for drug delivery in cancer therapy, J. Mater. Chem. B. 1 (2013) 5742–5750. https://doi.org/10.1039/c3tb21176b.

[20] Z. Shen, G. Reznikoff, G. Dranoff, K.L. Rock, Cloned dendritic cells can present exogenous antigens on both MHC class I and class II molecules., J. Immunol. 158 (1997) 2723–30. http://www.ncbi.nlm.nih.gov/pubmed/9058806.

[21] J.D. Pfeifer, M.J. Wick, R.L. Roberts, K. Findlay, S.J. Normark, C. V. Harding, Phagocytic processing of bacterial antigens for class I MHC presentation to T cells,

Nature. 361 (1993) 359–362. https://doi.org/10.1038/361359a0.

[22] H. Sigmundsdottir, J. Pan, G.F. Debes, C. Alt, A. Habtezion, D. Soler, E.C. Butcher, DCs metabolize sunlight-induced vitamin D3 to “program” T cell attraction to the epidermal chemokine CCL27, Nat. Immunol. 8 (2007) 285–293. https://doi.org/10.1038/ni1433.

[23] W. Dawicki, C. Li, J. Town, X. Zhang, J.R. Gordon, Therapeutic reversal of food allergen sensitivity by mature retinoic acid–differentiated dendritic cell induction of LAG3+CD49b−Foxp3− regulatory T cells, J. Allergy Clin. Immunol. 139 (2017) 1608-1620.e3. https://doi.org/10.1016/j.jaci.2016.07.042.

[24] K.A. Wojtal, L. Wolfram, I. Frey-Wagner, S. Lang, M. Scharl, S.R. Vavricka, G. Rogler, The effects of vitamin A on cells of innate immunity in vitro, Toxicol. Vitr. 27 (2013) 1525–1532. https://doi.org/10.1016/j.tiv.2013.03.013.

[25] Y. Qiang, J. Xu, C. Yan, H. Jin, T. Xiao, N. Yan, L. Zhou, H. An, X. Zhou, Q. Shao, S. Xia, Butyrate and retinoic acid imprint mucosal-like dendritic cell development synergistically from bone marrow cells, Clin. Exp. Immunol. 189 (2017) 290–297. https://doi.org/10.1111/cei.12990.

[26] T. Feng, Y. Cong, H. Qin, E.N. Benveniste, C.O. Elson, Generation of Mucosal Dendritic Cells from Bone Marrow Reveals a Critical Role of Retinoic Acid, J. Immunol. 185 (2010) 5915–5925. https://doi.org/10.4049/jimmunol.1001233.

[27] L. Saurer, K.C. McCullough, A. Summerfield, In Vitro Induction of Mucosa-Type Dendritic Cells by All- Trans Retinoic Acid , J. Immunol. 179 (2007) 3504–3514. https://doi.org/10.4049/jimmunol.179.6.3504.

[28] D. Liang, A. Zuo, H. Shao, W.K. Born, R.L. O’Brien, H.J. Kaplan, D. Sun, Retinoic acid inhibits CD25+ dendritic cell expansion and γδ T-cell activation in experimental autoimmune uveitis., Invest. Ophthalmol. Vis. Sci. 54 (2013) 3493–3503. https://doi.org/10.1167/iovs.12-11432.

[29] L. Abdelhamid, H. Hussein, M. Ghanem, N. Eissa, Retinoic acid-mediated anti-inflammatory responses in equine immune cells stimulated by LPS and allogeneic mesenchymal stem cells, Res. Vet. Sci. 114 (2017) 225–232. https://doi.org/10.1016/j.rvsc.2017.05.006.

[30] H. Torres-Aguilar, M. Blank, L.J. Jara, Y. Shoenfeld, Tolerogenic dendritic cells in autoimmune diseases. Crucial players in induction and prevention of autoimmunity, Autoimmun. Rev. 10 (2010) 8–17. https://doi.org/10.1016/j.autrev.2010.07.015.

CHAPTER 3

Protection of gut microbiome from antibiotics: development of a vancomycin-specific adsorbent with high adsorption capacity

3.1. Introduction

Antibiotics are used extensively for the treatment of infectious diseases. However, during antibiotic treatment, the non-absorbed fraction of orally administered antibiotics, along with the fraction excreted into the upper intestine via bile of both orally and parenterally administered antibiotics, reaches the large intestine where it affects the gut microbiome to induce dysbiosis [1]. Dysbiosis in the gut microbiome results in various consequences in the short and long term, including *Clostridioides difficile* infection (CDI) [2], the generation of antibiotic-resistant bacteria [3], allergies, and metabolic syndromes [4].

To avoid gut dysbiosis induced by antibiotics, strategies to protect the gut microbiome during antibiotic treatment need to be developed. Two strategies have been reported to date. One of these strategies is the oral administration of β-lactamase to degrade residual β-lactam antibiotics that reach the large intestine [5–8]. It has been reported recently that a clinical trial of this therapy for the suppression of antibiotic-induced CDI was successful [9]. However, this therapy is only applicable to β-lactam antibiotics. The other reported strategy to protect the gut microbiome is using activated charcoal (AC) as an adsorbent of antibiotics in the large intestine [10,11]. Utilizing nonspecificity in adsorption of hydrophobic molecules, AC is potentially applicable to a variety of antibiotics. However, the nonspecific characteristics of AC pose the risk of side

effects; they may affect the metabolism of host animals by the nonspecific adsorption of biological compounds in the intestinal fluid, such as bile acids and essential micronutrients. In the treatment of patients with renal failure, orally administered AC nonspecifically adsorbed bile acids [12], which is suspected to be a risk factor for cardiovascular disease [13]. It was reported that AC did not change the amount of necessary trace metal ions such as iron, zinc and manganese in the digestive tract in animal study [14]. Thus, as for metal ions, such AC's adverse effect may not be a concern. To avoid the nonspecific adsorption of biological compounds in the upper intestine, colon-specific AC has been developed in which AC was coated with pectin, which is degradable by colonic microflora [15]. A phase I clinical trial of this AC formulation showed that the fecal free-antibiotic level was reduced to a negligible level, without affecting the blood concentration of some biological compounds [10]. Capturing orally administered antibiotics by AC before reaching to intestine, where antibiotics is adsorbed, should be avoided. Thus, giving enough interval between the administration of antibiotics and AC would work to avoid this issue. AC administration at least 2 hours before or 1 hour after the oral administration of antibiotics would avoid the removal of antibiotics in upper gastrointestinal tract.

Here, we sought to develop specific adsorbents for antibiotics, free from the risks associated with nonspecific adsorbents (Fig. 1). As a target antibiotic, we selected vancomycin (VCM), which is used widely against Gram-positive bacteria. VCM treatment via both oral and parenteral administration causes gut dysbiosis [16,17], as well as generating VCM-resistant bacteria colonies in the rectum [18]. VCM specifically binds to the carboxyl-terminus of peptidoglycan precursors terminating in the sequence D-Ala-D-Ala-OH to block the cross-linking reaction in the growing bacterial cell wall [19]. We used this peptide as a ligand to adsorb VCM. It has been reported that cell-wall mimetic peptides, such as *N,N'*-diacetyl-L-Lys-D-Ala-D-Ala-OH have a relatively high binding

affinity to VCM (dissociation constant K_d = 10^6 M^{-1}) [20]. To immobilize the peptide ligand, we used a crosslinked polymeric support for the solid phase peptide synthesis because it enables high loading of the ligand peptide. A high ligand content is important to achieve adsorption of VCM in the large intestine using a practical dosage. To raise the loading of the ligand in the microparticles (MPs), the ligand was attached to the MPs via a linker of dendritic D-lysine [21] (Fig. 1b). Using the obtained ligand-modified MPs, we investigated the adsorption of VCM *in vivo*, and the suppression of CDI in a mouse model.

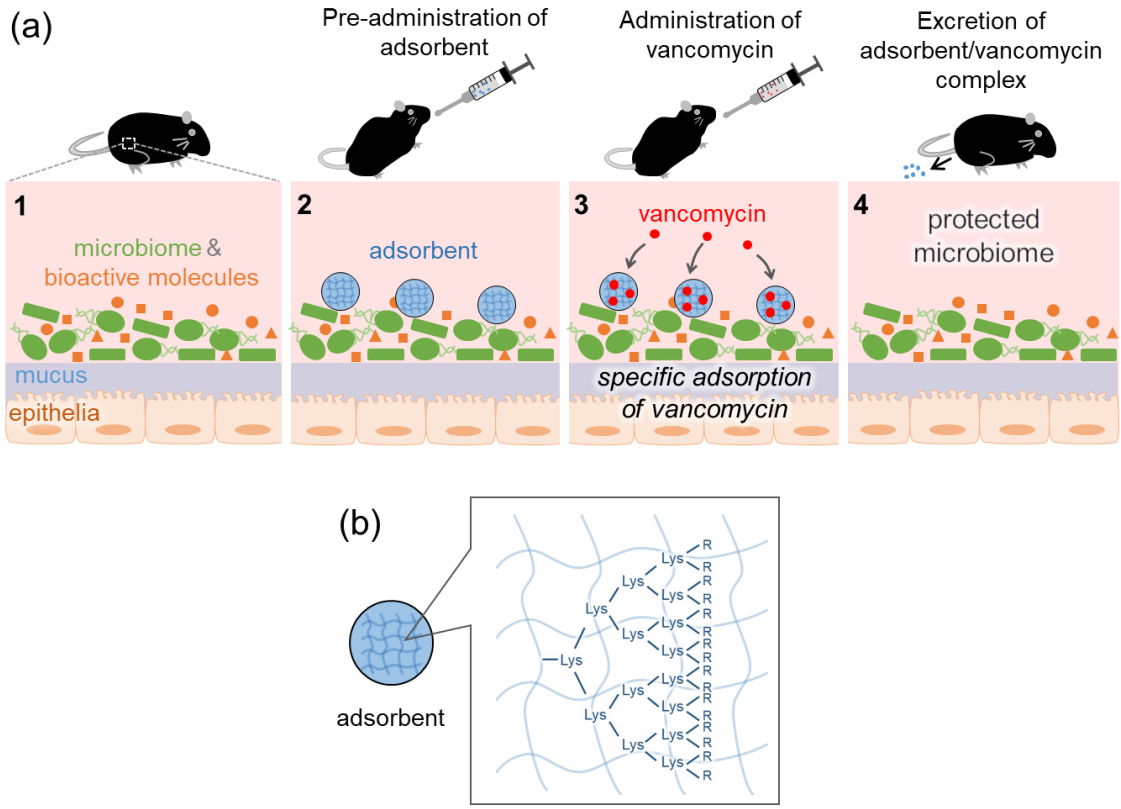

Fig. 3.1. (a) Mechanism of action of the VCM-specific adsorbent MPs in the large intestine. Pre-administered adsorbent specifically captures VCM and protects the gut microbiome and minimizes the effect on the concentrations of bioactive molecules in the intestinal fluid. (b) Schematic drawing of a MP. The MP is a spherical hydrogel of crosslinked polyethyleneglycol with the VCM-specific ligand (D-Ala-D-Ala-OH) immobilized via D-lysine dendrons. R indicates the ligand.

3.2. Materials and Methods

3.2.1. Preparation of MPs

D-Lysine dendrons terminated with the ligand were synthesized on NovaPEG amino resin (0.2 mmol of amine group) by Fmoc solid-phase peptide synthesis (SPPS) and tert-butyl SPPS for the D-lysine dendron and ligand, respectively. First, the D-lysine dendron was synthesized using Fmoc-D-Lys(Fmoc)-OH and N-[1-(cyano-2-ethoxy-2-oxoethylideneaminooxy) dimethylamino(morpholino)] uronium hexafluorophosphate (COMU) as the carboxyl-group activating agent. Then, succinic anhydride was attached to the lysine α and ε-amine groups using DMAP followed by addition of Fmoc-L-Lys-OH•HCl using COMU. After removing the Fmoc group, the α-amine group of L-lysine was acetylated with acetic anhydride. The amount of cleaved Fmoc groups were used to quantify the number of modified L-lysine resides. H-D-Ala-OtBu was attached to the α-carboxyl group of lysine using COMU. After removing the tert-butyl group using trifluoroacetic acid/dichloromethane = 9:1, addition of H-D-Ala-OtBu and removal of the tert-butyl group were repeated. After completion of the reaction, the resin was washed with tetrahydrofuran MeOH, water, and citrate buffer (pH 3.0) and dried in a desiccator.

3.2.2. Field emission scanning electron microscope observations

Dried MPs were placed on carbon sheets and their morphology was observed by Field Emission Scanning Electron Microscope (SEM) (Hitachi SU8000, Japan) operated at 10 kV.

3.2.3. Adsorption of VCM to MPs

VCM (1.0–50 μg/mL), and swelled MPs (2.0 mg) obtained by incubation for 24 h at 37°C in distilled water were mixed in 500 μL of phosphate buffered salts (PBS) (pH 7.4) and

shaken (200 rpm) in a shaker for 24 h at r.t. Then the concentration of VCM in the aqueous phase was determined by high performance liquid chromatography (HPLC). VCM was quantified by a HPLC validated method using an Elite Lachrom L2455 diode array detector (Hitachi, Japan) on a COSMOSIL 5C4 column (5 μm, 10 × 150 mm). An isocratic mobile phase consisting of 10% methanol and 90% milli-Q water was used with a flow rate of 1.0 mL/min and a 50 μL injection volume. VCM was detected at a wavelength of 225 nm. The adsorption isotherm was fitted based on the Langmuir equation as follows using Prism 8 (GraphPad Software):

$$C_e/Q_e = K_d/Q_m + C_e/Q_m$$

where C_e (M) is the equilibrium concentration of VCM in solution, Q_e (mol-VCM/g-MPs) is the amount of VCM adsorbed at equilibrium, Q_m (mol-VCM/g-MPs) is the adsorption capacity of the MPs, and K_d (M) is the dissociation constant.

3.2.4. Evaluation of the minimal inhibitory concentration 50 value

Swelled MPs in MD12 medium (500 μL) were added into the top compartment of transwells (3 μm porosity; BD Biosciences) in 6-well plates (Corning). *Staphylococcus lentus* isolate in the logarithmic growth period was added to MD12 medium and incubated at 37°C for 24 h. Then, the 50-μL suspensions were mixed with the VCM-containing MD12 medium and the mixtures (1.5 mL) were applied gently into the bottom compartment of the transwells. Then, the plates were incubated at 37°C for 24 h in a constant temperature incubator. The minimal inhibitory concentration (MIC) value was determined as the lowest VCM concentration to show no growth of turbidity with the plate reader at a wavelength of 600 nm. The MIC50 value was defined as the lowest concentration of VCM at which 50% of the bacteria were inhibited.

3.2.5. Determination of the dose of MPs in vivo

CB57/BL6 mice (male; 8 weeks-old) were purchased from Kyudo Co., Ltd. (Saga, Japan). Animal experiments were performed according to the guidelines for animal care and use committee, Kyushu University. Mice were fed with 30 kGy γ-irradiated CE-2 (CLEA Japan Inc.), with access to bedding and tap water. Mice had a cycle of 12 h of light and 12 h of darkness. For *in vivo* capacity testing, mice (n = 3) were administered MP-G4 (3.0 or 10.0 mg/100 μL Dulbecco's phosphate-buffered saline (DPBS)), and after 1 h, VCM (300 μg/100 μL sterile water) was administered by oral gavage. The feces were collected over 23 h after administration. Distilled water was then added to 1.0 g of a feces sample and the dispersion was vortex mixed. The dispersion was centrifuged at 8,000 rpm for 10 min at 4°C. The supernatant was then filtered through a 0.45 μm filter and diluted with mobile phase before being analyzed using HPLC. The HPLC analysis procedure was the same as that described in Section 2.2.3. To examine the effect of repeated daily treatments, mice were divided into four groups (n = 3 per group) and administered either DPBS or MP-G4 (10.0 mg/100 μL DPBS), and after 1 h, either sterile water or VCM (300 μg/100 μL sterile water) by oral gavage. The treatment was conducted once a day for 7 days and body weight was measured daily.

3.2.6. *C.difficile* spore preparation

C. difficile VPI10463 (ATCC 43255) spores were prepared as follows. *C. difficile* VPI10463 was grown overnight in 5 mL of Columbia Broth at 37ºC under anaerobic conditions. The next day, 40 mL of Clospore media was added to the inoculum. The culture media was anaerobically incubated at 37ºC for 7 days. Spores were harvested by centrifugation and washed with cold water three times. Spore stocks were stored at 4ºC in sterile water. Viable spores were enumerated by plating for colony-forming unit (CFU)/mL on taurocholate, cefoxitin, cycloserine, fructose agar (TCCFA) to determine

the challenge dose.

3.2.7. VCM and MP administration and challenge with *C. difficile*

C57BL/6J WT mice (female; 5-weeks old) were purchased from CLEA Japan Inc. Mice were fed with 30 kGy γ-irradiated CE-2 (CLEA Japan Inc.), with access to bedding and tap water. Mice had a cycle of 12 h of light and 12 h of darkness. The procedure for the animal experiment is shown in Figure S1. The C57BL/6J WT mice (female; 5-weeks old) were divided into four groups (n = 6 per group) and administered DPBS(-) or MP-G4 (10.0 mg/100 μL DPBS), and after 1 h, either sterile water or vancomycin (300 μg/100 μL sterile water) was administered by oral gavage for 5 days (= treatment period). Following the treatment period, mice were allowed to drink normal water for 2 days, and the next day, mice were challenged with *C. difficile* spores 1 x 10^4 CFU by oral gavage. These animal experiments were conducted using protocols approved by Keio University Ethics Committee for Animal Experiments.

3.2.8. 16s ribosomal DNA analysis

Mouse fecal samples were collected and preserved at –80ºC. Bacterial DNA was extracted complying with the E.Z.N.A. Stool DNA Kit Pathogen Detection protocol (OMEGA). The V3-V4 region of the 16S rDNA gene was amplified following DNA extraction using universal primers (Table S1). The PCR reaction mixture consisted of 5 ng/μL of DNA extraction mix, 2.5 μL; 2 × CAPA HiFi mix (Illumina), 12.5 μL; and 1 μM of each primer, 5 μL. The cycling conditions were: 95ºC (3 min), 25 cycles of 95ºC (30 s), 55ºC (30 s), and 72ºC (30 s) followed by a final elongation step at 72ºC (5 min). The amplicon DNA were purified using AMPure XP beads (Beckman Coulter) followed by a second PCR reaction with a mixture consisting of purified DNA, 5 μL; 2 × CAPA HiFi mix (Illumina), 25 μL; distilled water 10 μL; and 1 μM of each primer, Nextera XT

index kit (Illumina), 5 μL. The cycling conditions were: 95ºC (3 min), 8 cycles of 95ºC (30 s), 55ºC (30 s), and 72ºC (30 s) followed by a final elongation step at 72ºC (5 min). Likewise, tagged DNA were purified with AMPure XP beads, and diluted in 10 mM Tris-HCl buffer (pH 8.5) to 12 pM and all samples were pooled. The completed library was sequenced on an Illumina Miseq 600 cycle V3-V4 kit (Illumina).

3.2.9. Evaluation of fecal CFU

C. difficile CFUs were determined using fecal samples collected on day 1 after infection. Fecal samples were weighed and suspended in 1 mL of DPBS (-) and homogenized in the anaerobic chamber. An aliquot (50 μL) of the suspensions were plated 50 μL on TCCFA and incubated at 37ºC under anaerobic conditions for 3 days. Then, the number of colonies were enumerated.

3.2.10. ELISA of fecal lipocalin-2

Feces collected on day 1 after infection were weighed and stored at –80ºC. The fecal samples were suspended in DPBS (-) containing 0.1% Tween-20 (100 mg/mL), and vortexed for 20 min. The suspension was centrifuged at 12,000 rpm, 4ºC, for 10 min[1]. The ELISA was conducted according to the protocol of the ELISA kit (R&D Systems, DY1857). Samples were diluted in the kit-recommended reagent diluent [1% BSA in DPBS (-)].

3.2.11. Statistical analysis

Statistical analyses were performed using R studio (Version 1.1.456). The survival rate and significance between the four groups were tested by the Kaplan-Meier test using R Survival package. Bartlett's test was used to determine significance of variance between the four groups. If the differences were significant ($p < 0.05$), Scheffe's test was used for

comparisons of discontinuous variables between the four groups. The Tukey HSD test was used for comparisons between the four groups with similar variance. The diversity of the gut microbiota was analyzed by QIIME13 and R using R vegan and multcomp packages. Intra- and inter-group β-diversity analysis was analyzed by R using R multcomp package. * $p < 0.05$, ** $p < 0.01$, *** $p < 0.001$.

3.3. Results and Discussion

3.3.1. Preparation of ligand-modified MPs

A dendritic ligand unit was synthesized by SPPS on commercially available resin (Fig. 3.2). Here, we used water-swellable NovaPEG amino resin that is composed of crosslinked PEG [22] as water-swellable properties are a prerequisite for the adsorption of VCM in the intestinal fluid. First, 3rd or 4th generation $_{D}$-lysine dendron units were synthesized on the resin using Fmoc-$_{D}$-Lys(Fmoc)-OH as the monomer. $_{D}$-Lysine was employed here for its resistance against peptidases in the gastrointestinal fluid. Then, the α- and ε-amine groups of terminal $_{D}$-lysine residues were converted to carboxyl groups using succinic anhydride (Scheme S1). On the carboxyl groups, ε-$_{L}$-lysine was introduced, then the ligand ($_{D}$-Ala-$_{D}$-Ala-OH) was synthesized using H-$_{D}$-Ala-OtBu as the monomer via *tert*-butyl SPPS [23]. Before modification of H-$_{D}$-Ala-OtBu, the number of terminal $_{L}$-lysine residues was quantified from the amount of Fmoc groups released from the terminal $_{L}$-lysine, and the yield for this step based on the number of initial amine groups in the resin was calculated (yield in Table 3.1). The yield became lower with increasing generations probably because of the steric repulsion in the crowded termini of the dendrons of higher generations. Indeed, 4th generation is reported to be the maximum for quantitative preparation [24]. The amount of loaded ligand per weight of MP was not very different between MP-G3 and MP-G4 (Table 3.1) because most of the total weight of these MPs was the weight of the dendritic ligand unit (68% for MP-G3 and 83% for MP-G4).

SEM images of each dry MP showed that a spherical shape was maintained even for the high weight fraction of the dendritic ligand unit (Fig. 3.3). MPs with higher generation dendrons had a larger size, reflecting the increase of the weight fraction of the dendritic ligand unit with each generation. The size of the MP (> 100 μm) was sufficient to avoid

penetrating the intestinal epithelium [24].

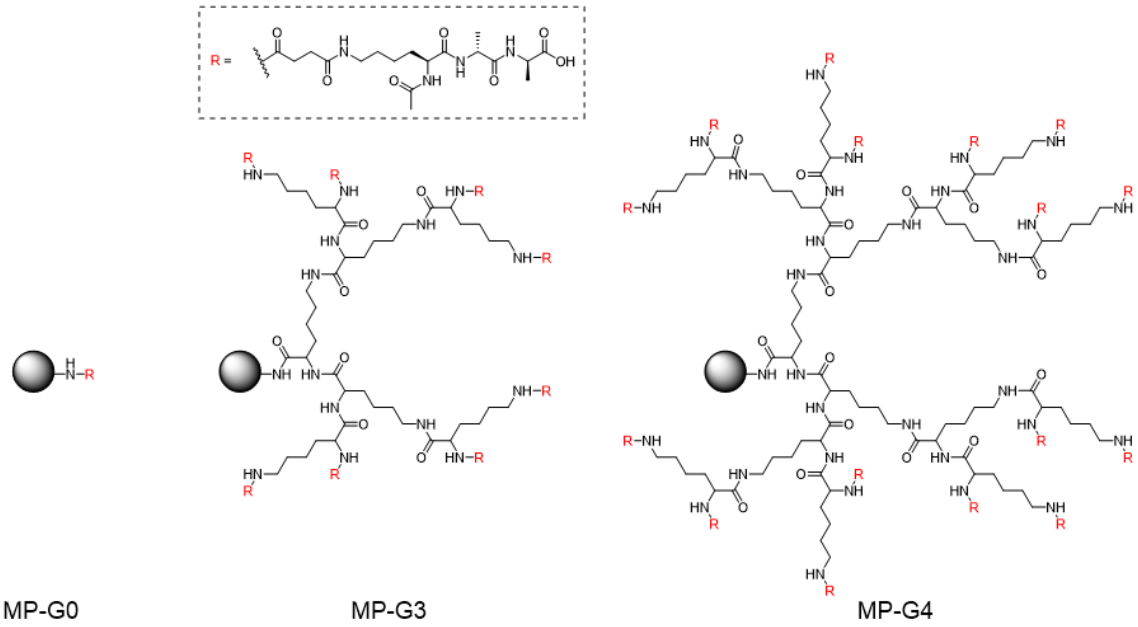

Fig. 3.2. Chemical structures of the ligand-modified MPs with three levels of dendritic ligand generations. Spheres indicate the matrix of resin.

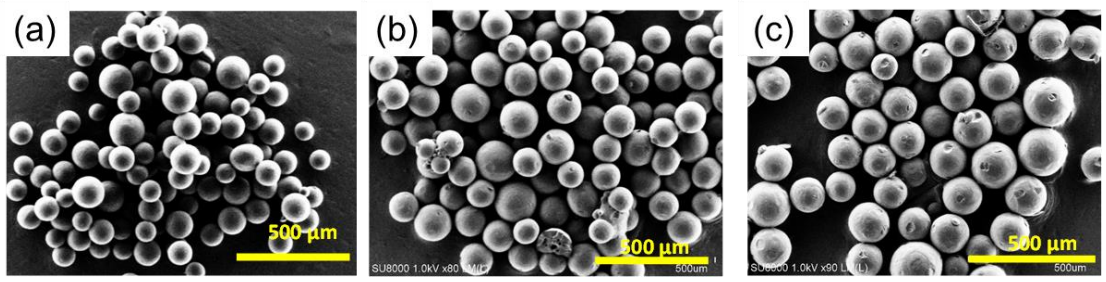

Fig. 3.3. SEM images of ligand-modified MPs. (a) MP-G0, (b) MP-G3, and (c) MP-G4. Scale bars show 500 µm.

Table 3.1. Characteristics of MPs.

	MP-G0	MP-G3	MP-G4
yield [%] [a]	100	58	42
loaded ligand [μmol/mg]	0.44	1.1	1.2
diameter [μm][b]	111 ± 20	139 ± 24	150 ± 31
Q_{max} [μmol/mg]	0.24	0.35	0.35
$Q_{max,g}$ [g/g]	0.36	0.51	0.51
$Q_{max,mol}$ [mol/mol]	0.86	0.46	0.41
K_d [μM]	14	29	20

[a]: Overall yield until the modification of L-lysine residue.

[b]: Determined from SEM image

3.3.2. Adsorption of VCM to MPs

The adsorption characteristics of the ligand-modified MPs toward VCM were evaluated. After incubating a mixture of each MP and VCM for 24 h at 37°C, unbound VCM was quantified using HPLC. The adsorption isotherms of each MP are summarized in Fig. 3.4. Intact NovaPEG amino resin (naked MP; NP in Fig. 3.4) showed negligible adsorption of VCM. In contrast, the ligand-modified MPs showed adsorption of VCM depending on the generation level, indicating the specific interaction of the ligand of the MPs with VCM. The maximum adsorption amount (Q_{max}) and dissociation constant (K_d) were calculated using the Langmuir equation and are summarized in Table 1. The K_d values were not affected by the generation level of the dendron unit. The Q_{max} values of

the MPs with dendritic ligands were higher than that of MP-G0, but the increments were smaller than the values expected from the loaded ligand. The $Q_{max,mol}$ value, which is a stoichiometric expression of Q_{max}, showed that only half of the ligands in MP-G3 and MP-G4 functioned to capture VCM, indicating that the sterically crowded state of the ligands on the dendrons will impede the recognition of VCM. Typical Q_{max} values of AC for various antibiotics are reported to be 10^{-1} to 10^{0} g/g [26]. Thus, the Q_{max} values of the MPs were equivalent to those of AC, a representative adsorbent with a high capacity. Compared with the reported K_d value of a complex between a free ligand and VCM (~1 μM) [27], the K_d values of the MPs were one order of magnitude higher. The lower affinity of the ligands in the MPs compared with the free ligand can be explained by the aforementioned result that half of the ligands cannot bind VCM because of steric hindrance. We also confirmed specificity of MP-G4 to VCM over other antibiotics (cefoperazone, clarithromycin) (Fig. 3.5). We found that MP-G4 specifically adsorbed VCM, while AC as a control adsorbed cefoperazone and clarithromycin by nonspecific hydrophobic interaction. Thus, MP-G4 is specific adsorbent for VCM.

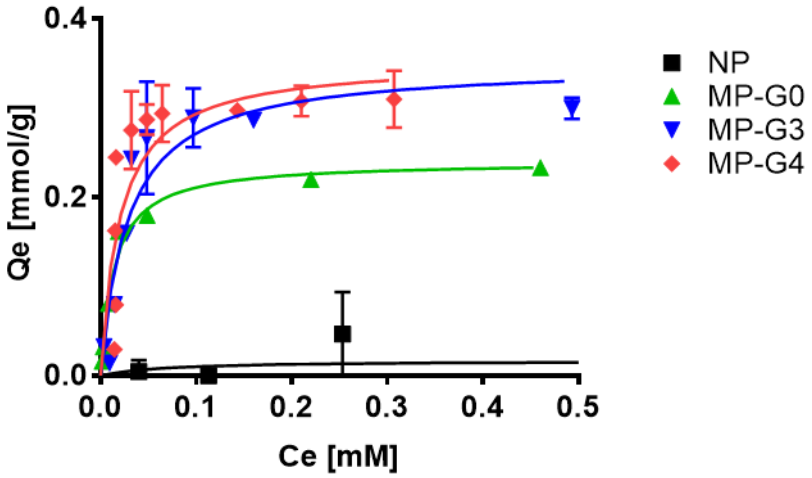

Fig. 3.4. Adsorption isotherms of VCM to the MPs. VCM and MPs (4.0 mg/mL) were mixed in PBS (pH 7.4) and incubated for 24 h at r.t. The concentration of free

VCM was determined by HPLC.

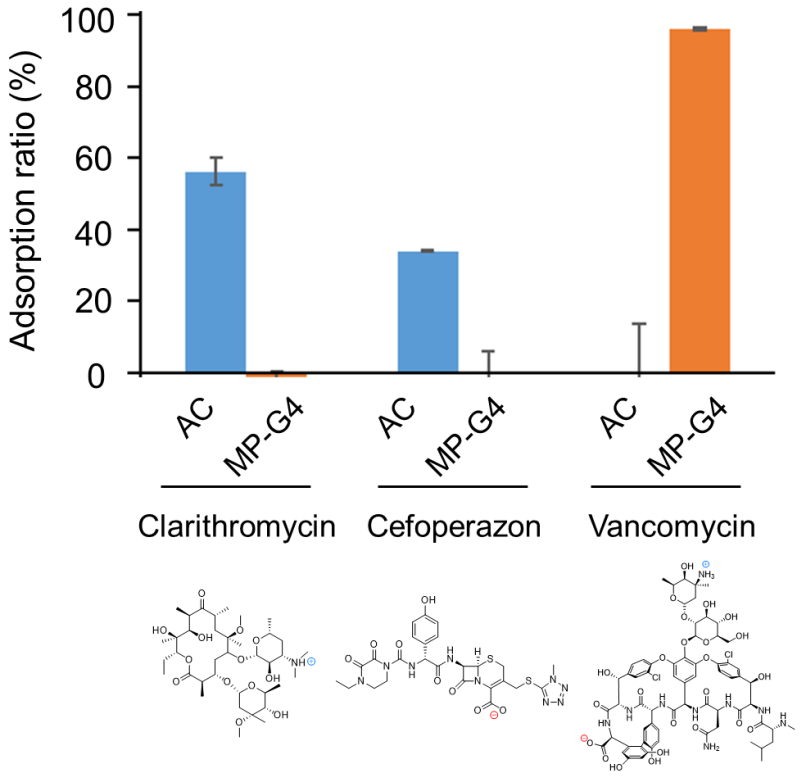

Fig. 3.5. Adsorption of antibiotics to MP-G4 and AC. Experimental procedures were same with those of VCM adsorption to MPs described in Materials and Methods section. Concentration of each antibiotic was 350 μM. Amount of MP-G4 or AC was 2.0 mg. Hydration of MP-G4 or AC (purchased from UES, Japan) was conducted in distilled water for 24 h at 37°C in distilled water.

The ability of the MPs to protect bacteria from VCM was determined from the MIC50 value. The Gram-positive bacteria, *S. lentus* was cultured in the presence of VCM and each MP for 24 h. As shown in Fig. 3.6a, the MIC50 value of VCM toward *S. lentus* was 6.0 μg/mL in the absence of MPs, which is consistent with the reported value [22]. Naked MPs (NP) showed almost no effect on the MIC50 value, while the ligand-modified

MPs clearly raised the MIC50 values; the MIC50 values in the presence of MP-G3 and MP-G4 were 33 and 63 μg/mL, respectively. MP-G4 showed a slightly higher protective effect than MP-G3. Fig. 3.6b shows the concentration dependence of the protective effect of MP-G4. The MIC50 value correlated with the concentration of MP-G4. These results showed ability of the MPs to protect bacteria from VCM.

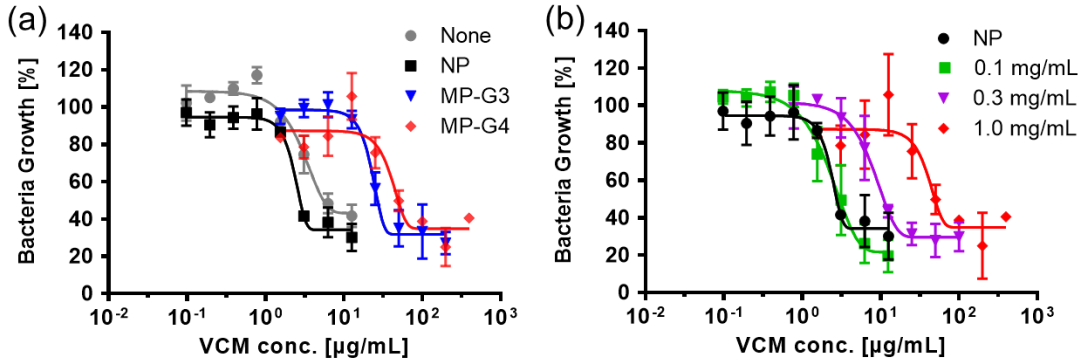

Fig. 3.6. Protection of *S. lentus* from VCM by different MPs (a) and by MP-G4 at different concentrations (b). *S. lentus* was incubated in MD12 medium containing VCM with or without MPs (1.0 mg/mL in panel a) at 37°C for 24 h. The MIC50 value was determined from the turbidity at 600 nm. Data are represented by the mean ± SD (n = 3).

3.3.3. Adsorption of VCM to MPs in vivo to protect the microbiome

The required dosage of MP-G4 to capture VCM in the gastrointestinal tract was determined. First, MP-G4 was administered by oral gavage. After 1 h (during this period, microparticles start to reach the cecum [28,29]), VCM (300 μg) was administered orally. After VCM administration, the feces were collected over 23 h and the amount of free VCM in the feces was quantified by HPLC analysis. As shown in Fig. 3.6a, without the pre-administration of MP-G4, approximately 70% of orally administered VCM was detected in the feces. In the presence of MP-G4, the amount of VCM in the feces was

reduced in a dose-dependent manner. A dosage of 10.0 mg of MP-G4 was found to be sufficient to capture all the VCM; thus, hereafter, we used a 10.0 mg dosage of MP-G4. The binding capacity of MP-G4 calculated from 3.0 mg of MP-G4 was 0.023 mg/mg. Though this value is one order of magnitude lower than the binding capacity determined in PBS shown in Fig. 3.4 (0.51 mg/mg), the VCM adsorption efficacy of MP-G4 appears to be high. This is desirable considering the presence of a large amount of biological compounds in the gastrointestinal fluid that will compete with VCM in binding with the ligand. According to the dose conversion equation based on the surface area and body weight [29], the calculated dosage of MP-G4 for human application would be 40.5 mg/kg, which is comparable with the dosage of pectin-coated AC in a clinical trial (7.5 g/human; 125 mg/kg) [10]. When this administration regimen was conducted once a day for 7 days in mice, no detectable loss of body weight was observed (Fig. 3.6b).

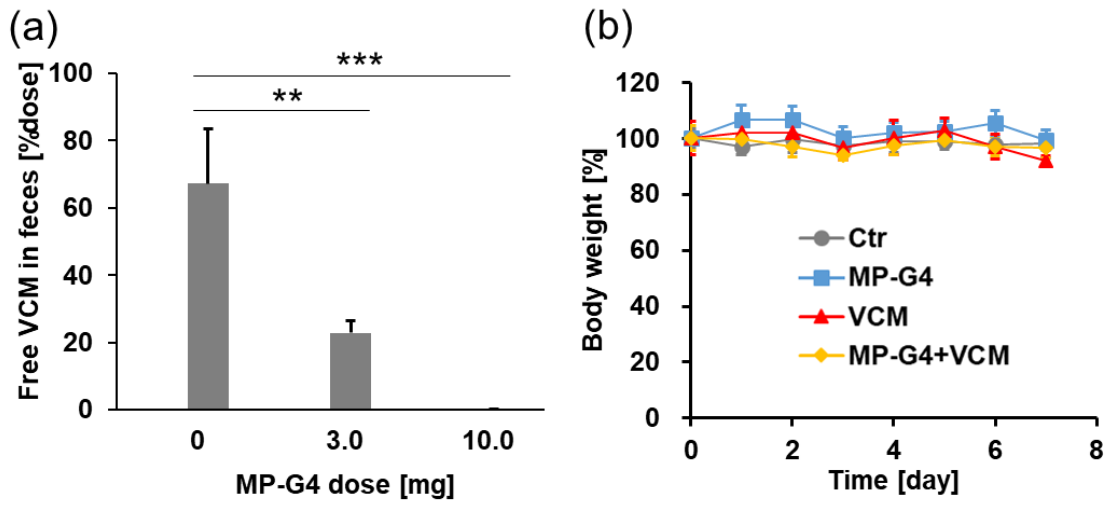

Fig. 3.7. (a) Amount of free VCM in the feces of mice orally treated with VCM and MP-G4 (n = 3 per group). **p < 0.01, ***p < 0.001. VCM (300 µg/100 µL) was administered 1 h after MP-G4 (0–10.0 mg/100 µL). (b) The body weight change in the four groups of mice (n = 3 per group) treated once a day for 7 days.

To examine whether pre-administration of MP-G4 could prevent VCM-induced gut dysbiosis *in vivo*, we analyzed gut microbiota composition before and after VCM (300 μg) treatment by 16S rDNA sequencing. The composition of gut microbiota was not different between all the groups before treatment, but changed significantly after VCM treatment. The administration of MP-G4 did not affect the gut microbial community. Pre-administration of MP-G4 prevented changes in gut microbial composition induced by VCM treatment (Fig. 3.8a). Specifically, the abundance of Enterobacteriales and Erysipelotrichales was significantly increased in the VCM-treated group compared with the control group. In contrast, this increase in the abundance of these bacteria was not observed in the VCM-treated group pre-administered with MP-G4 (Fig. 3.8b).

VCM is active against most Gram-positive bacteria and causes the overgrowth of Enterobacteriales in the gut [17,30]. In general, a bloom of Enterobacteriales is a hallmark of gut dysbiosis [31]. Therefore, our results indicated that the pre-administration of MP-G4 protected the gut microbiota from VCM-induced dysbiosis by capturing VCM in the gastrointestinal tract.

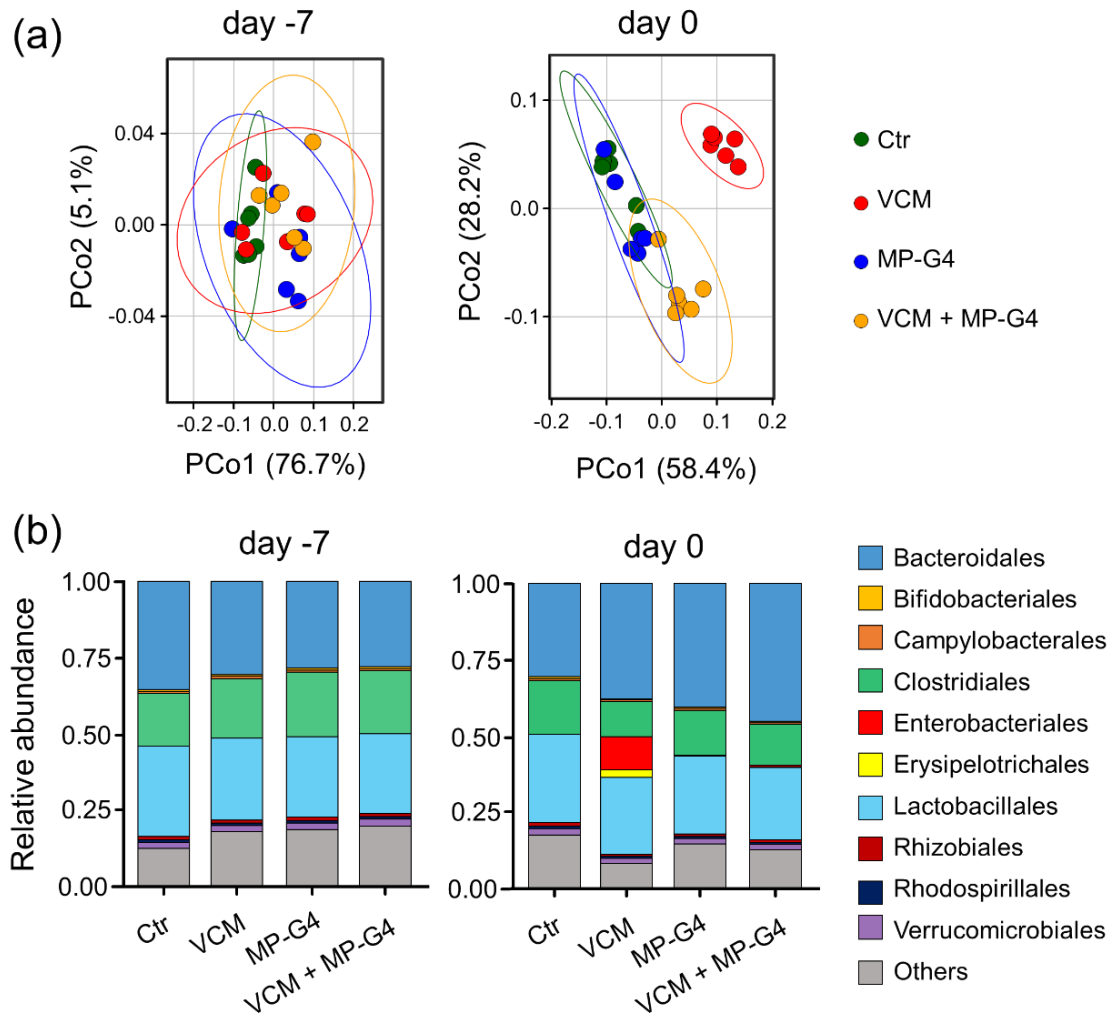

Fig. 3.8. Pre-administration of MP-G4 prevented VCM-induced perturbation in gut microbiota. (a) Principal coordinates analysis plot of weighted-Unifrac distances by water (Ctr), VCM, MP-G4, or VCM with MP-G4-treated groups (n = 6 per group). (b) Fecal microbiota composition of mice orally treated with water (Ctr), VCM, MP-G4, or VCM with MP-G4 on day –7 (just before treatment) and day 0 (after treatment) (n = 6 per group). Each bar shows the mean of individual mice from each group.

3.3.4. Protection from *C. difficile* infection

Disruption of the gut microbiota induced by the use of antibiotics enables *C. difficile* colonization in the gut [32]. In particular, an increase in the abundance of Enterobacteriales is associated with higher susceptibility to *C. difficile* colonization [32,33]. Therefore, we next investigated whether the pre-administration of MP-G4 protected VCM-treated mice against CDI. While all the control mice survived, VCM-treated mice all succumbed to CDI on the second day post-infection. However, both the VCM-treated or -untreated mice, pre-administered with MP-G4, all survived post CDI (Fig. 3.9a). *C. difficile* reached ~10^8 CFU/g feces 1 day post infection in the VCM-treated mice. In contrast, the burden of *C. difficile* in the feces of both the control and VCM-treated mice, pre-administered with MP-G4, as well as in the control mice was not detectable (< 10^2) or under 10^5 CFU/g feces (Fig. 3.9b). Furthermore, the level of lipocalin-2, an antimicrobial protein released from the epithelia in inflammation [35], increased in the VCM-treated mice but not in the control mice nor in the control and VCM-treated mice, pre-administered with MP-G4 (Fig. 3.9c). These results indicated that the pre-administration of MP-G4 protected VCM-treated mice against CDI.

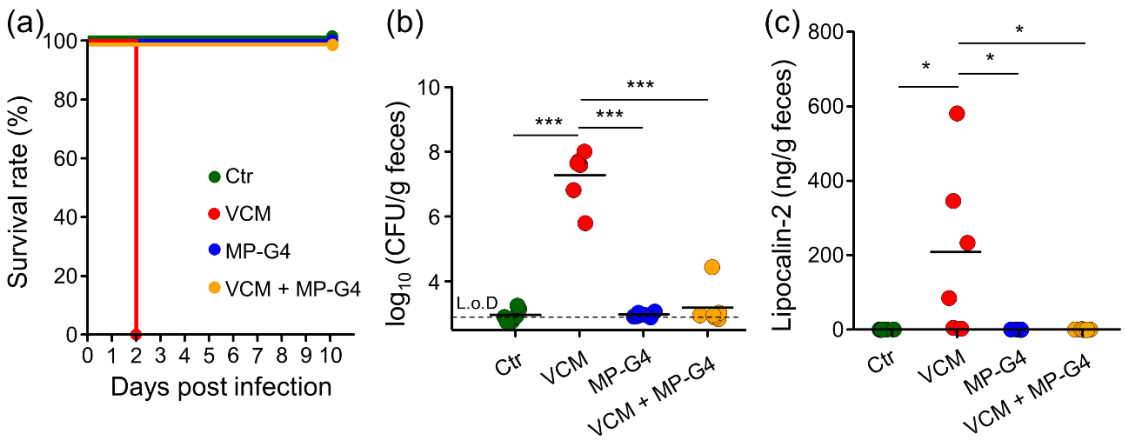

Fig. 3.9. Pre-administration of MP-G4 protected VCM-treated mice against CDI. (a) Mouse survival over time after CDI of C57BL/6J female mice treated with water (Ctr),

MP-G4, VCM, or VCM with MP-G4 (n = 6 per group). (b) Pathogen loads [CFU/g] in feces were detected 1 day after infection. Each dot represents an individual mouse. L.o.D = limit of detection. (c) ELISA measurement of lipocalin-2 in feces from *C. difficile*-infected mice from each group. (n = 6 per group). * $p < 0.05$, *** $p < 0.001$.

3.4. Conclusions

We proposed the use of antibiotic-specific adsorbents to protect the gut microbiome from VCM-induced dysbiosis. We prepared adsorbent MPs composed of hydrogels of crosslinked PEG with a specific peptide ligand to VCM immobilized via dendritic D-lysine as a linker to achieve a high content of the ligand in the MPs. The prepared MPs showed a relatively high capacity for VCM adsorption in aqueous media (~0.5 g/g). This is equivalent to the reported capacity toward various antibiotics of activated charcoal, which is a representative nonspecific adsorbent. *In vitro* tests showed that the MPs improved the resistance of *S. lentus* toward VCM. After oral administration at a practical dosage, MP-G4 adsorbed VCM in the intestine almost completely and suppressed dysbiosis of the gut microbiome in mice. As a consequence of the protection from gut dysbiosis, the mice were resistant against an oral challenge with the spores of *C. difficile*. These promising features of MPs indicate that MPs have the potential to be a new class of specific adsorbents to protect the gut microbiome during VCM treatment, without interfering with the metabolism of host animals.

3.5. References

[1] L. Dethlefsen, D.A. Relman, Incomplete recovery and individualized responses of the human distal gut microbiota to repeated antibiotic perturbation, Proc. Natl. Acad. Sci. U. S. A. 108 (2011) 4554–4561. https://doi.org/10.1073/pnas.1000087107.

[2] C.M. Theriot, V.B. Young, Interactions Between the Gastrointestinal Microbiome and Clostridium difficile , Annu. Rev. Microbiol. 69 (2015) 445–461. https://doi.org/10.1146/annurev-micro-091014-104115.

[3] S. Burtion, N. Washington, R.J.C. Steele, R.M.A.L. Feely, Intragastric Distribution of Ion-exchange Resins: a Drug Delivery System for the Topical Treatment of the Gastric Mucosa, J. Pharm. Pharmacol. 47 (1995) 901–906. https://doi.org/10.1111/j.2042-7158.1995.tb03268.x.

[4] Y. Belkaid, T.W. Hand, Role of the microbiota in immunity and inflammation, Cell. 157 (2014) 121–141. https://doi.org/10.1016/j.cell.2014.03.011.

[5] J. Harmoinen, K. Vaali, P. Koski, K. Syrjänen, O. Laitinen, K. Lindevall, E. Westermarck, Enzymic degradatoin of a β-lactam antibiotic, ampicillin, in the gut: A novel treatment modality, J. Antimicrob. Chemother. 51 (2003) 361–365. https://doi.org/10.1093/jac/dkg095.

[6] J. Harmoinen, S. Mentula, M. Heikkilä, M. Van Der Rest, P.J. Rajala-Schultz, C.J. Donskey, R. Frias, P. Koski, N. Wickstrand, H. Jousimies-Somer, E. Westermarck, K. Lindevall, Orally Administered Targeted Recombinant Beta-Lactamase Prevents Ampicillin-Induced Selective Pressure on the Gut Microbiota: A Novel Approach to Reducing Antimicrobial Resistance, Antimicrob. Agents Chemother. 48 (2004) 75–79. https://doi.org/10.1128/AAC.48.1.75-79.2004.

[7] U. Stiefel, J. Harmoinen, P. Koski, S. Kääriäinen, N. Wickstrand, K. Lindevall, N.J. Pultz, R.A. Bonomo, M.S. Helfand, C.J. Donskey, Orally administered

recombinant metallo-β-lactamase preserves colonization resistance of piperacillin-tazobactam-treated mice [2], Antimicrob. Agents Chemother. 49 (2005) 5190–5191. https://doi.org/10.1128/AAC.49.12.5190-5191.2005.

[8] A. Hoffman, E. Horwitz, S. Hess, R. Cohen-Poradosu, L. Kleinberg, A. Edelberg, M. Shapiro, Implications on emergence of antimicrobial resistance as a critical aspect in the design of oral sustained release delivery systems of antimicrobials, Pharm. Res. 25 (2008) 667–671. https://doi.org/10.1007/s11095-007-9373-6.

[9] J.F. Kokai-Kun, T. Roberts, O. Coughlin, C. Le, H. Whalen, R. Stevenson, V.J. Wacher, J. Sliman, Use of ribaxamase (SYN-004), a β-lactamase, to prevent Clostridium difficile infection in β-lactam-treated patients: a double-blind, phase 2b, randomised placebo-controlled trial, Lancet Infect. Dis. 19 (2019) 487–496. https://doi.org/10.1016/S1473-3099(18)30731-X.

[10] J. De Gunzburg, A. Ghozlane, A. Ducher, E. Le Chatelier, X. Duval, E. Ruppé, L. Armand-Lefevre, F. Sablier-Gallis, C. Burdet, L. Alavoine, E. Chachaty, V. Augustin, M. Varastet, F. Levenez, S. Kennedy, N. Pons, F. Mentré, A. Andremont, Protection of the human gut microbiome from antibiotics, J. Infect. Dis. 217 (2018) 628–636. https://doi.org/10.1093/infdis/jix604.

[11] J. De Gunzburg, A. Ducher, C. Modess, D. Wegner, S. Oswald, J. Dressman, V. Augustin, C. Feger, A. Andremont, W. Weitschies, W. Siegmund, Targeted adsorption of molecules in the colon with the novel adsorbent-based Medicinal Product, DAV132: A proof of concept study in healthy subjects, J. Clin. Pharmacol. 55 (2015) 10–16. https://doi.org/10.1002/jcph.359.

[12] Y. Araki, T. Tsujikawa, A. Andoh, M. Sasaki, Y. Fujiyama, T. Bamba, Therapeutic effects of an oral adsorbent on acute dextran sulphate sodium-induced colitis and its recovery phase in rats, especially effects of elimination of bile acids in gut lumen, Dig. Liver Dis. 32 (2000) 691–698. https://doi.org/10.1016/S1590-

8658(00)80332-1.

[13] Y. Liu, J. Coresh, J.A. Eustace, J.C. Longenecker, B. Jaar, N.E. Fink, R.P. Tracy, N.R. Powe, M.J. Klag, Association between Cholesterol Level and Mortality in Dialysis Patients: Role of Inflammation and Malnutrition, J. Am. Med. Assoc. 291 (2004) 451–459. https://doi.org/10.1001/jama.291.4.451.

[14] K. M. Wilson, Evaluating the Aaddition of Charcoals to Broiler Diets on the Recovery of Salmonella Typhimurium Grow-out and Processing, The University of Georgia, 2014, Master thesis

Y. Liu, J. Coresh, J.A. Eustace, J.C. Longenecker, B. Jaar, N.E. Fink, R.P. Tracy, N.R. Powe, M.J. Klag, Association between Cholesterol Level and Mortality in Dialysis Patients: Role of Inflammation and Malnutrition, J. Am. Med. Assoc. 291 (2004) 451–459. https://doi.org/10.1001/jama.291.4.451.

[15] M. Khoder, N. Tsapis, V. Domergue-Dupont, C. Gueutin, E. Fattal, Removal of residual colonic ciprofloxacin in the rat by activated charcoal entrapped within zinc-pectinate beads, Eur. J. Pharm. Sci. 41 (2010) 281–288. https://doi.org/10.1016/j.ejps.2010.06.018.

[16] A.L. Halpin, T.J.B. de Man, C.S. Kraft, K.A. Perry, A.W. Chan, S. Lieu, J. Mikell, B.M. Limbago, L.C. McDonald, Intestinal microbiome disruption in patients in a long-term acute care hospital: A case for development of microbiome disruption indices to improve infection prevention, Am. J. Infect. Control. 44 (2016) 830–836. https://doi.org/10.1016/j.ajic.2016.01.003.

[17] L. Sun, X. Zhang, Y. Zhang, K. Zheng, Q. Xiang, N. Chen, Z. Chen, N. Zhang, J. Zhu, Q. He, Antibiotic-induced disruption of gut microbiota alters local metabolomes and immune responses, Front. Cell. Infect. Microbiol. 9 (2019) 1–13. https://doi.org/10.3389/fcimb.2019.00099.

[18] C.J. Donskey, M.S. Helfand, N.J. Pultz, L.B. Rice, Effect of Parenteral

Fluoroquinolone Administration on Persistence of Vancomycin-Resistant Enterococcus faecium in the Mouse Gastrointestinal Tract, Antimicrob. Agents Chemother. 48 (2004) 326–328. https://doi.org/10.1128/AAC.48.1.326-328.2004.

[19] G.M. Sheldrick, P.G. Jones, O. Kennard, D.H. Williams, G.A. Smith, Structure of vancomycin and its complex with acetyl-D-alanyl-D-alanine, Nature. 271 (1978) 223–225. https://doi.org/10.1038/271223a0.

[20] R. Kannan, C.M. Harris, T.M. Harris, J.P. Waltho, N.J. Skelton, D.H. Williams, Function of the amino sugar and N-terminal amino acid of the antibiotic vancomycin in its complexation with cell wall peptides, J. Am. Chem. Soc. 110 (1988) 2946–2953. https://doi.org/10.1021/ja00217a042.

[21] V. Swali, N.J. Wells, G.J. Langley, M. Bradley, Solid-Phase Dendrimer Synthesis and the Generation of Super-High-Loading Resin Beads for Combinatorial Chemistry, J. Org. Chem. 62 (1997) 4902–4903. https://doi.org/10.1021/jo9708654.

[22] W.M. Cho, B.P. Joshi, H. Cho, K.H. Lee, Design and synthesis of novel antibacterial peptide-resin conjugates, Bioorganic Med. Chem. Lett. 17 (2007) 5772–5776. https://doi.org/10.1016/j.bmcl.2007.08.056.

[23] W.G. Gutheil, X.U. Qingchai, N-to-C solid-phase peptide and peptide trifluoromethylketone synthesis using amino acid tert-butyl esters, Chem. Pharm. Bull. 50 (2002) 688–691. https://doi.org/10.1248/cpb.50.688.

[24] G. Fischer, B. Wängler, C. Wängler, Optimized solid phase-assisted synthesis of dendrons applicable as scaffolds for radiolabeled bioactive multivalent compounds intended for molecular imaging, Molecules. 19 (2014) 6952–6974. https://doi.org/10.3390/molecules19066952.

[25] C. Schmidt, C. Lautenschlaeger, E.M. Collnot, M. Schumann, C. Bojarski, J.D. Schulzke, C.M. Lehr, A. Stallmach, Nano- and microscaled particles for drug

targeting to inflamed intestinal mucosa - A first in vivo study in human patients, J. Control. Release. 165 (2013) 139–145. https://doi.org/10.1016/j.jconrel.2012.10.019.

[26] M.J. Ahmed, Adsorption of quinolone, tetracycline, and penicillin antibiotics from aqueous solution using activated carbons: Review, Environ. Toxicol. Pharmacol. 50 (2017) 1–10. https://doi.org/10.1016/j.etap.2017.01.004.

[27] R. Jianghong, Y. Lin, L. Joydeep, G.M. Whitesides, R.M. Weis, H.S. Warren, Binding of a dimeric derivative of vancomycin to L-Lys-D-Ala-D-lactate in solution and at a surface, Chem. Biol. 6 (1999) 353–359. https://doi.org/10.1016/S1074-5521(99)80047-7.

[28] G.M. Hodges, E.A. Carr, R.A. Hazzard, K.E. Carr, Uptake and translocation of microparticles in small intestine - Morphology and quantification of particle distribution, Dig. Dis. Sci. 40 (1995) 967–975. https://doi.org/10.1007/BF02064184.

[29] P. Padmanabhan, J. Grosse, A.B.M.A. Asad, G.K. Radda, X. Golay, Gastrointestinal transit measurements in mice with 99mTc-DTPA-labeled activated charcoal using NanoSPECT-CT, EJNMMI Res. 3 (2013) 1. https://doi.org/10.1186/2191-219X-3-60.

[30] C. Walsh, 4 Walsh, 406 (2000) 775–781. www.nature.com.

[31] M.Y. Zeng, N. Inohara, G. Nuñez, Mechanisms of inflammation-driven bacterial dysbiosis in the gut, Mucosal Immunol. 10 (2017) 18–26. https://doi.org/10.1038/mi.2016.75.

[32] A.M. Seekatz, V.B. Young, Clostridium difficile and the microbiota, J. Clin. Invest. 124 (2014) 4182–4189. https://doi.org/10.1172/JCI72336.

[33] D.E. Freedberg, N.C. Toussaint, S.P. Chen, A.J. Ratner, S. Whittier, T.C. Wang, H.H. Wang, J.A. Abrams, Proton Pump Inhibitors Alter Specific Taxa in the

Human Gastrointestinal Microbiome: A Crossover Trial, Gastroenterology. 149 (2015) 883-885.e9. https://doi.org/10.1053/j.gastro.2015.06.043.

[34] L. Zhang, D. Dong, C. Jiang, Z. Li, X. Wang, Y. Peng, Insight into alteration of gut microbiota in Clostridium difficile infection and asymptomatic C. difficile colonization, Anaerobe. 34 (2015) 1–7. https://doi.org/10.1016/j.anaerobe.2015.03.008.

[35] B. Chassaing, G. Srinivasan, M.A. Delgado, A.N. Young, A.T. Gewirtz, M. Vijay-Kumar, Fecal Lipocalin 2, a Sensitive and Broadly Dynamic Non-Invasive Biomarker for Intestinal Inflammation, PLoS One. 7 (2012) 3–10. https://doi.org/10.1371/journal.pone.0044328.

CHAPTURE 4

General Conclusions

Increase in the patient of diseases related to the disruption of immunological homeostasis is threatening issue worldwide. Many reasons have been proposed for the increment of the disruption of immunological homeostasis. One of the reasons is the dysbiosis of the intestinal microbiome which is caused by administration of antibiotics. To restore the disrupted immunological homeostasis, immunotherapy using an antigen is fundamental solution. However, usually this kind of therapy (desensitization) takes time for completion. In this paper, I approached the goal in two ways to maintain or restore the immunological homeostasis.

In Chapter 2, I developed vitamin-peptide conjugates as effective inducer of immunotolerance toward the antigen peptides. Here I selected ATRA and vD3 as inducer of tolerogenic dendritic cells. Selective modification of these vitamins on the N-terminus of the peptide was achieved by the scheme I developed here. The obtained conjugates showed the functions of both vitamins and antigen peptides, i.e., anti-inflammatory effects resulting from ATRA and activation of antigen-specific T cells. The conjugates reported here can be expected to promote the induction of antigen-specific Tregs, which is essential to restore the disruption of immunological homeostasis.

In Chapter 3, I proposed an antibiotic-specific adsorbent to prevent dysbiosis caused by antibiotic treatment. Hydrophilic polyethyleneglycol-based microparticles were modified with peptide ligands in a high density which is a vancomycin-specific ligand. The microparticles showed high capacity and specificity to vancomycin and successfully captured vancomycin in vivo. The microparticles protected from the C. difficile infection induced by vancomycin-induced dysbiosis.

Perspectives

In this thesis, we developed materials to maintain immunological homeostasis. I found that vitamin-peptide conjugates can be expected to induce antigen-specific immune tolerance. I have clarified the importance of antibiotic-specific adsorbents for protection of the intestinal microbiome. These findings will lead to the development of more practical materials to prevent and maintain disruption of immunological homeostasis.

The peptide immunotherapy for allergy uses multiple antigenic peptides. The synthetic scheme of conjugates we developed here is generally applicable any peptide sequences. As a formulation to deliver these conjugates, liposome may be useful. The ATRA-peptide conjugates are highly hydrophobic and can be inserted into the lipid bilayer of liposomes. Therefore, by inserting the conjugates into the liposome bilayer membrane, it becomes possible to simultaneously deliver multiple antigenic peptides and ATRA to dendritic cells. One of the problems of the conjugates will be the low availability of ATRA and the peptides probably due to the low cleavage efficiency of the conjugate by endosomal peptidases. Thus, using environment-responsive cleavable linker such as a disulfide bond may overcome the problem.

The adsorbent using an antibiotic-specific ligand showed high specificity and capacity, and prevented vancomycin-induced dysbiosis. For antibiotics to which the ligands are difficult to design, molecular imprint polymers (MIPs) will be useful as ligands. MIPs can be prepared easily by using antibiotics as templates, and MIPs usually has high affinity and specificity to the target molecules. By using MIPs as specific adsorbents for various antibiotic, prevention of dysbiosis by the antibiotics can be expected.

Accomplishments

List of oral presentation

1. 「アレルゲン特異的な免疫治療を目指したビタミン-ペプチドコンジュゲートの創製」、第 40 回日本バイオマテリアル学会大会、2018 年 11 月
2. 「腸内細菌叢を保護するバンコマイシン選択的捕捉レジンの開発」、第 35 回日本 DDS 学会学術集会、2018 年 7 月
3. 「抗原特異的な免疫寛容の誘導を目指したビタミン-ペプチドコンジュゲートの創製」、第 41 回日本バイオマテリアル学会、2019 年 11 月

List of poster presentation

1. 「アレルギー治療に向けたリン脂質被膜ポリ乳酸ナノ粒子の開発」、九州地区高分子若手研究会・冬の講演会 2015、2015 年 12 月
2. 「炎症性腸疾患の治療に向けた脂質被覆粒子の開発」、日本バイオマテリアル学会シンポジウム 2016、2016 年 11 月
3. 「腸内マクロファージを標的とする免疫抑制性ナノ粒子の開発」、第 49 回若手ペプチド夏の勉強会、2017 年 8 月

4. 「慢性炎症の治療を目指した脂質自己供給型ナノ粒子の開発」、第 66 回高分子学会年次大会、2017 年 5 月

List of international poster presentations

5. 「Development of phosphatidylserine containing nanoparticle suppression inflammation」、The 11th SPSJ International Polymer Conference、2016 年 12 月
6. 「Development of Self-Filling Nanoparticle for Suppression of Inflammatory」、biomaterials international 2017、2017 年 8 月

List of publication

1. **Kazuki Yuzuriha**, Kyosuke Yakabe, Haruka Nagai1, Shunyi Li, Takeshi Zendo, Khadijah Zai, Akihiro Kishimura, Koji Hase, Yun-Gi Kim, Takeshi Mori, Yoshiki Katayama, “Protection of gut microbiome from antibiotics: development of a vancomycin-specific adsorbent with high adsorption capacity”, *Bioscience of Microbiota, Food and Health, in press.*
2. Kazuki Yuzuriha, Ayaka Yoshida, Shunyi Li, Akihiro Kishimura, Takeshi Mori, Yoshiki Katayama, “Synthesis of peptide conjugates with vitamins for induction of antigen-specific immunotolerance”, *Journal of Peptide Science*, submitted.

List of supplementary publication

1. Md. Zahangir Hosain, **Kazuki Yuzuriha**, Khadijah, Masafumi Takeo, Akihiro Kishimura, Yoshihiko Murakami, Takeshi Mori, Yoshiki Katayama, "Synergic modulation of inflammatory state of macrophages utilizing anti-oxidant and phosphatidylserine containing polymerlipid hybrid nanoparticles", *Med. Chem. Commun.,* **8**, 1514-1520 (2017).

2. Khadijah Zai, **Kazuki Yuzuriha**, Akihiro Kishimura, Takeshi Mori, Yoshiki Katayama, "Preparation of Complexes between Ovalbumin Nanoparticles and Retinoic Acid for Efficient Induction of Tolerogenic Dendritic Cells", *Analytical Sciences,* **34**, 1243-1248 (2018).

Acknowledgments

Completion of this research work and dissertation could not be achieved without the assistance, cooperation and understanding of multiple people.

First and foremost, I wish to thank my supervisor Professor Yoshiki Katayama for his sustained support during the three years. Under his guidance and advisory I was able to solve difficultness that I was facing during my experimental and research path. To me, his constant understanding and back up was always the greatest motivation to be able to keep doing my best and going forward.

Special mention goes to my research advisor, Associate Professor Takeshi Mori. It has been an honor to be his first Ph.D. student from Immunity group. He has taught me, both consciously and unconsciously, how to be good researcher. I appreciate all his contributions of time and ideas to make my Ph.D. experience productive and stimulating. I am thankful to him as he patiently taught me the correct way of making advanced presentations or writing decent scientific papers, which were accompanied with reminding me many subtle yet important points.

I would like to express my sincere thanks to Associate Professor Akihiro Kishimura for his valuable advice on my experimental procedures during discussions and presentations.

I am deeply grateful for the collaborative assistance of Professor Koji Hase and Professor Yu-Gi Kim also his students (Mr. Yakabe kyosuke, Mr. Kinashi Yusuke,). Professor Koji Hase generously provided me with his methodological knowledge and Prof. Hase's team supported me in animal experiment, which was a critical part in my research hypothesis.

I would also like to express my special thanks to my research fellows, Immunity group, Khadijah, Yunmei Mu, Ayaka Yoshida, Haruka Nagai, and Li Shunyi, Li Shintei, Kurumi Matsuo for the discussion times that I had over my research ideas.

My sincere thanks to all my doctoral thesis committee members, Professor Noriho Kamiya and Professor Noritada Kaji for their time and invaluable advice on my thesis project.

My fruitful educational stay in the prestigious Kyushu University and Katayama laboratory could not be realized without the financial support from Graduate education and research training program in DECISION SCIENCE for sustainable society, which I am greatly appreciative.

Lastly, I would like to thank my family for all their love and encouragement. For my parents who raised me with a love and supported me in all my pursuits. And also my brother-sisters for their compassionate support throughout my study in abroad.

Kazuki Yuzuriha

Kyushu University

March, 2020